REVISED CLEAN Manuscript: Canadian Journal of Earth Sciences Special Issue: *Uniformitarianism and Plate Tectonics: A tribute to Kevin C. Burke and John F. Dewey* (February 2016)

Earth Evolution and Dynamics – A tribute to Kevin Burke

Trond H. Torsvik[1-3], Bernhard Steinberger[4,1], Lewis D. Ashwal[3], Pavel V. Doubrovine[1], Reidar G. Trønnes[1,5]

[1]Centre for Earth Evolution and Dynamics (CEED), University of Oslo, 0316 Oslo, Norway; [2]Geodynamics, NGU, N-7491 Trondheim, Norway; [3]School of Geosciences, University of Witwatersrand, WITS 2050, South Africa; [4]GFZ German Research Centre for Geosciences, 14473 Potsdam, Germany; [5]Natural History Museum, University of Oslo, 0318 Oslo, Norway.

Abstract

Kevin Burke's original and thought-provoking contributions have been published steadily for the past sixty years, and more than a decade ago he set out to resolve how plate tectonics and mantle plumes interact by proposing a simple conceptual model, which we will refer to as "the Burkian Earth". On the Burkian Earth, mantle plumes take us from the deepest mantle to sub-lithospheric depths, where partial melting occurs, and to the surface, where hotspot lavas erupt today, and where large igneous provinces and kimberlites have erupted episodically in the past. The arrival of a plume head contributes to continental break-up and punctuates plate tectonics by creating and modifying plate boundaries. Conversely, plate tectonics makes an essential contribution to the mantle through subduction. Slabs restore mass to the lowermost mantle and are the triggering mechanism for plumes that rise from the margins of large-scale low shear-wave velocity structures in the lowermost mantle, that Kevin christened TUZO and JASON. Situated just above the core-mantle boundary beneath Africa and the Pacific, these are two stable and antipodal thermochemical piles, which Kevin reasons represent the immediate after-effect of the moon-forming event and the final magma ocean crystallization.

Keywords: Plate Tectonics, Large Igneous Provinces, Mantle Plumes, Deep Earth

Introduction

Kevin Burke's fundamental and enduring contribution to the Earth Sciences is the scholarly analysis of the extent to which the tectonics of the present-day Earth can be applied to the history of the planet. Kevin defines tectonics as "the large scale evolution of planetary lithospheres", and the hypothesis he has evaluated throughout his career is that plate tectonics has been the dominant terrestrial heat-loss mechanism throughout geologic time.

Kevin coined the term "Wilson Cycle" for the sequence of continental rifting, ocean opening, subduction and ocean closure, and final continent-continent collision (Wilson, 1966). He quickly recognized that the continents would hold the record of plate interaction in deep time and in the early 1970s in collaboration with John Dewey, he wrote a series of papers (e.g. Burke and Dewey 1973, Dewey and Burke 1973) that fundamentally changed the way we think about the formation of continental lithosphere in general and Precambrian lithosphere in particular. Kevin was a pioneer in suggesting that Precambrian orogens like the Grenville are the eroded products of Himalayan-style collisions. He also proposed in the early 1970's that greenstone belts, present in nearly all Archean regions, are allochthonous volcano-sedimentary packages originally formed as marginal basins, ocean islands, and arcs and were later thrust onto older continents. Kevin also spent a large part of his career working on the geology of the Caribbean region, but here we focus on his more recent visions on how large igneous provinces at the Earth's surface may have originated as plumes from the edges of the seismically slower and stable parts of the deepest mantle.

Since 1953 Kevin has had numerous teaching and lecturing positions in several continents, but perhaps his most important position was as professor and chairman of the Geology Department at SUNY Albany (1973-1982). The Department that he put together and the science that emerged in that period had a profound influence on the evolution of geological thought.

Kevin's presence at scientific meetings is legendary. Many of us have watched Kevin sit in the front row of a session and proceed to stimulate the often-reticent audience into animated discussion. In addition, he never allows a missing speaker to derail a good session and he has occupied many unscheduled vacancies by delivering his own ideas and questions and encouraging discussions.

Hotspots and Mantle Plumes

Tuzo Wilson at the University of Toronto suggested in 1963 that linear chains of seamounts and volcanoes — which display an age progression — are caused by relatively small areas of melting in the mantle, termed hotspots. Jason Morgan later proposed that hotspots may be caused by mantle plumes up-welling from the lower mantle and constructed the first hotspot reference frame in 1971. Kevin met and worked with Tuzo in the early 1970s, a turning point in his career. Together they published four papers in Nature (Burke and Wilson 1972, Wilson and Burke 1972, Burke et al. 1973a,b) and later a review paper on *Hotspots on the Earth's surface* in Scientific American (Burke and Wilson 1976). Hotspots are commonly referred to as volcanism unrelated to plate boundaries and rifts. A few also lie at the ends of volcano chains connected to Large Igneous Provinces (LIPs), e.g. the Tristan (Paraná-Etendeka) and Reunion (Deccan) hotspots. The Hawaiian hotspot may also have been linked to a now subducted LIP, whilst the New England hotspot lies at the end of a trail that was connected with Jurassic kimberlite volcanism in continental North-East America (Zurevinski et al. 2011). An excellent summary describing the dynamic processes linking hotspots, mantle plumes and LIPs can be found in Duncan and Richards (1991).

In 2003 Kevin enthusiastically arrived in Trondheim, Norway, to share his latest visions on the origin of LIPs. Kevin had plotted reconstructed LIP eruption centres based on palaeogeographic maps by Eldholm and Coffin (2000) and Scotese et al. (1987) on a seismic shear-wave model map of Li and Romanowicz (1996; SAW12D), representing the mantle velocity structure directly above the Core-Mantle Boundary (CMB). Here he had made the key observation that most LIPs — when erupted — lay near the radial projections onto the Earth's surface of the margins of the low-velocity shear-wave regions of the D" zone just above the CMB. His ideas were first published in Burke and Torsvik (2004), who demonstrated that the majority of reconstructed LIPs of the past 200 Myr plot within or overlay the edges of two low-velocity regions near the CMB (Fig. 1a). These two equatorial and antipodal regions — argued to be the most probable sources of the mantle plumes that generated LIPs — were dubbed *Sub-African* and *Sub-Pacific* regions, later Large Low Shear-wave Velocity Provinces (LLSVPs, Garnero et al. 2007), or simply TUZO and JASON by Burke (2011). The pattern observed by Burke and Torsvik (2004) implied that TUZO and JASON must have been fairly stable in their present location at least since the eruption of the Central Atlantic Igneous Province (marked C in Fig. 1a) near the Triassic-Jurassic boundary.

Observations

Burke and Torsvik (2004) originally restored 25 LIPs of the past 200 Myr to their eruption sites, using a global palaeomagnetic reference model, and they introduced the 'zero-longitude' Africa approach in order to constrain longitude semi-quantitatively from palaeomagnetic data. The largest uncertainty in their procedure arose in reconstructing seven Cretaceous Pacific LIPs in the African palaeomagnetic frame using relative plate circuits. Nonetheless, the majority of LIPs — when erupted — lay above TUZO and JASON (Fig. 1a). Clear exceptions, however, were the youngest and smallest LIP, the Columbia River Basalt in the Western United States (ca. 15 Ma), the Maud Rise offshore East Antarctica (in that paper thought to be 73 Ma), and the Manihiki Plateau.

In a follow-up paper, Torsvik et al. (2006) tested four different plate motion reference frames (African fixed hotspot, African moving hotspot, Global moving hotspot and Global Palaeomagnetic) to restore LIPs to their eruption sites. They also compared the reconstructed positions of LIPs with several global tomography models, mapped out the location of shear-wave velocity gradients near the CMB, and pointed out that most restored LIPs overly a contour of constant velocity that corresponds to the highest values of the horizontal velocity gradient. That contour — 1% slow contour in the SMEAN model (Fig. 1b) — was dubbed the Plume Generation Zone (PGZ) by Kevin in Burke et al. (2008). The 2006 model used a chain of relative motion, which connects Africa and the Pacific via East Antarctica–Australia–Lord Howe Rise for times between 46.3 and 83.5 Ma (plate circuit Model 2 of Steinberger et al., 2004). Prior to that, the Pacific Ocean LIPs in the global moving hotspot frame were restored with rotation rates derived from a less reliable fixed hotspot frame back to 150 Ma. Reconstructions of LIPs in the 2004 and 2006 models differ in detail because of different plate motion frames. Another key difference was the location of Maud Rise based on new marine magnetic data that had become available, which showed that the Maud Rise erupted close to 125 Ma, and not at 73 Ma. The revised age places the reconstructed Maud Rise (Fig. 1b) right on top of the margin of TUZO (1% slow contour in SMEAN). The analyses of reconstructed LIPs were also extended back to 251 Ma using the Siberian Traps; it is noteworthy that the Siberian Traps either overlie a smaller anomaly (~ -0.5%) in the lower mantle (later named Perm in Lekic et al. 2012; Fig. 2b) or a north-easterly arm of TUZO.

In 2010, reconstructions derived from a hotspot frame for the past 100 Myr were combined with a revised palaeomagnetic frame for older times (Torsvik et al. 2010) corrected for true polar wander (TPW; Steinberger and Torsvik 2008) between 320 and 100 Ma. This is known as the global hybrid frame (Torsvik et al. 2008*a*). TPW is the rotation of the crust and mantle relative to the spin axis. The paleomagnetic reconstructions reference the continents (and embedded LIPs) to the Earth's spin axis, and the deep mantle structures (LLSVPs) rotate with respect to the spin axis during the TPW events. Hence, in the correlative exercises illustrated in Figures 1 and 2, the paleomagnetic reconstructions should be corrected for TPW. Before 2008 we did not know how to do these corrections quantitatively, but the net cumulative effect of TPW since the Late Palaeozoic is at certain periods zero or otherwise small. Steinberger and Torsvik (2008) showed that TPW over the past 320 Myr consists of oscillations back and forth such that the pole never deviated by more than ~20° from its present position, and was within ~5° of the present position for about half of the time. Also, these oscillations occurred around an axis close to the LLSVP centres such that, regardless of whether the TPW rotations are considered or not, LIPs remain close to LLSVP margins. By 2010, LIP reconstructions were also extended back to the eruption of the Skagerrak Centred LIP (297 Ma, Torsvik et al. 2008*b*) in Northern Europe, dubbed SCLIP by Kevin Burke, the master of acronyms. We also extended Kevin's ideas of LIPs to kimberlites — igneous bodies thought to be caused by plumes heating thick cratonic lithosphere but not resulting in the formation of LIPs — and we demonstrated that more than 80% of all kimberlites for the past 320 Myrs also were sourced by plumes from near the edges of TUZO and JASON (Torsvik et al. 2010).

The correlation of reconstructed eruption sites of LIPs (Fig. 1) and kimberlites, at least since about 320 Ma when Pangea formed, indicates the long-term stability of TUZO and JASON. That remarkable correlation between surface and mantle features — as first envisioned by Kevin in 2003 — provides a novel way of reconstructing the longitudinal position of continents. Assuming that TUZO and JASON have remained nearly stationary before Pangea time, we can show that a geologically reasonable palaeogeographic model that reconstructs continents in *latitude* from palaeomagnetic data — and *longitude* in such a way that LIPs and kimberlites are positioned above the edges of TUZO and JASON at eruption times — can be defined for the entire Phanerozoic (Torsvik et al. 2014). We will refer to this procedure as the "plume generation zone reconstruction method". Figure 2a shows 31 reconstructed LIPs from Neogene (15 Ma) to Late Cambrian (510 Ma) times. Here we use a hybrid plate motion frame and only the Columbia River Basalts overlie regions of faster than average velocities in the deep mantle. The Ontong Java, Manihiki and Hikurangi LIPs were modelled as fragments of a single LIP (the Ontong Java Nui) formed at around 123 Ma (Chandler et al. 2012), and the Wallaby Plateau (originally 96 Myrs old) was assigned an age of 123 Ma after Olierook et al. (2015). About 1700 kimberlites show a similar pattern (Fig. 2b) as the LIPs (Fig. 2a), but Cretaceous-Tertiary kimberlites from NW America (as the Columbia River LIP) and Devonian kimberlites from Russia are notable exceptions that do not conform to this pattern.

Figure 3 shows three examples of global plate reconstruction from Late Triassic to Early Cretaceous times. Early Cretaceous kimberlites (Fig. 3a) are well known in South America-South Africa-Australia-East Antarctica, and they are mostly located near the margin of TUZO. Similarly, the reconstructed Maud Rise (125 Ma) and Rajasthan (118 Ma) LIPs plot near the TUZO margin whilst Ontong Java Nui (123 Ma) overlies the JASON margin. A similar pattern emerges for the Late Jurassic (Fig. 3b) with North American, NW African, South African and Australian kimberlites erupted over the TUZO margin. Late Jurassic kimberlites from Siberia, however, are not associated with the LLSVP margins (see also Heaman et al. 2015). Three Late Jurassic LIPs, Argo (155 Ma) and Magellan (145 Ma) and Shatsky (147 Ma) — the oldest known in-situ Oceanic LIPs — plot directly above the TUZO and JASON plume generation zones. The remarkable pattern of LIPs and kimberlites erupted above the TUZO-JASON margins is also evident for the Late Triassic-Early Jurassic; at that time kimberlites and one LIP (C, Central Magmatic Igneous Province) erupted above the entire length of the western margin of TUZO (Fig. 3c).

Geodynamic Models

The conclusions obtained in papers of Kevin Burke and co-authors that (*i*) plumes mainly form at the margins of LLSVPs, and that (*ii*) these margins are approximately stable through time promoted a number of numerical modelling experiments to reproduce and explain these features. Tan and Gurnis (2005) had already shown that if a chemically dense basal layer also has a higher bulk modulus than the surrounding mantle, it tends to form stable piles with steep edges. Due to their proximity to the hot core, these piles, while being chemically denser, are also hotter than the surrounding mantle and therefore nearly neutrally buoyant. In follow-up work, Tan et al. (2011) showed that plumes tend to preferentially, but not exclusively, form along the steep margins of such piles. Moreover the plumes from the margins, carrying material from near the hot core-mantle boundary to the surface, tend to have higher temperatures than those (fewer ones) forming at the tops of the piles. The mechanism invoked by Tan et al. (2011) to explain the "plumes from the margins" pattern is that subducted slabs "shape" thermochemical piles, but also push plumes towards the edges of these piles, where they remain. Tan et al. (2011) were interested in the long-term evolution over billions of years, and therefore did not prescribe subduction zone locations, as these are not known for such long timescales. In a complementary approach, Steinberger and Torsvik (2012) prescribed subduction zone locations, but initiated their calculation at 300 Ma, as no earlier subduction zone locations were available. In their model, plumes almost exclusively form at the margins of thermo-chemical piles, as slabs push both the basal chemical layer and hot material from the thermal boundary layer. In this way, hot piles of chemically distinct material are formed, and, as more hot material is pushed against their margins, it is forced to rise, forming mantle plumes. However, it can be suspected that the clear pattern found is partly a result of the relatively recent initiation of the model at 300 Ma. In order to test that, Steinberger and Torsvik (2012) re-initialized a model starting from the present-day structure and again imposing 300 Myr of subduction history. The resulting pattern then becomes less clear: Plumes are now also overlying pile interiors, but they still *initially form* mainly, but not exclusively, along their margins. Beyond this general pattern, Gaßmöller (2014) showed statistically significant correlations between modelled and actual mantle plume eruption sites. Similar results were also obtained by Hassan et al. (2015).

These and many other numerical models have in common that they assume a Newtonian viscous rheology for the mantle, whereby viscosity depends on pressure, and depth, and often also on temperature. This is a convenient assumption to keep the model relatively simple and tractable, but, at least for the lower mantle, a Newtonian rheology is also supported by experiments and observations. Karato and Li (1992) expected that diffusion creep should be the dominant deformation mechanism in lower mantle bridgmanite. This is also supported by the fact that seismic anisotropy, which would be expected if the alternative dislocation creep mechanism is dominant, is largely absent in the lower mantle, except at the base of the mantle near the edges of TUZO and the smaller Perm anomaly (Ford et al. 2015; Long and Lynner 2015). Hence the numerical models are characterized by large-scale flow in the lower mantle: Sinking slabs and rising plumes supply the main driving forces, but are also part of large convection cells. Accordingly, it can be expected that plumes get advected by this large-scale flow and become tilted and distorted (Steinberger and O'Connell 1998) unless they are located at positions of large-scale upwelling (Zhong et al. 2000).

However, the existence of such large-scale flow was never accepted by Kevin. In his view of the lower mantle (at least at depths where the influence of plate motions has ceased) only slabs sink and plumes rise vertically from the edges of thermo-chemical piles, accompanied by horizontal flow along the core-mantle boundary to satisfy mass conservation. Interestingly, French and Romanowicz (2015) showed in their tomography model that plumes are almost vertical below depths of about 1000 km. They take this as an indication that – apart from the plumes themselves – lower mantle flow may be rather sluggish. Alternatively, it may be an indication that the observed plumes occur at stagnation points of large-scale flow, as suggested by Zhong et al. (2000).

What is the reason for the absence, as envisioned by Kevin, of large-scale flow, predicted by numerical models? A concentration of deformation to zones of sinking slabs and rising plumes could be facilitated if the (effective) viscosity is strongly reduced in their vicinity. For slabs, this is contrary to expectation, as they are colder, hence expected to be more viscous, and coupled to and inducing flow in the surrounding mantle. Viscosity reduction could occur for non-linear stress-dependent rheology. But also in the case of Newtonian viscosity, it could be possible, if it strongly depends on grain size, and if the passage of slabs through the 660 km discontinuity is accompanied by grain size reduction. Such a grain size reduction accompanied by viscosity reduction has been proposed by Karato and Li (1992). Solomatov and Reese (2008) have explored the effect of grain size-dependent viscosity on large scale convection. Their *Figure 9* shows that low-viscosity slabs can still displace the chemical piles laterally and lead to strong heterogeneity in the mantle. Another effect that may lead to shear localization near subducted slabs would be a strong viscosity contrast between lower mantle constituents, bridgmanite and magnesiowüstite (Girard et al., 2016), if, under the stronger stresses surrounding slabs, the weak phase gets connected, whereas elsewhere the strong phase is interconnected. But until now, no numerical models of the mantle exist that would show the characteristics proposed by Kevin. Also, whole-mantle large-scale flow models have been very successful in explaining a number of observations, in particular the geoid (Hager and Richards 1989). Geoid highs above nearly neutrally buoyant LLSVPs can result from a hotter than average mantle above them to depths of about 1000 km (Figs. 2b, 4c) causing upward flow and surface deflection (dynamic topography). Before replacing these models, we should ascertain that proposed alternatives can also explain these observations. At the moment, it is not clear whether Kevin is right with his intuition, or rather the views prevalent in the numerical modelling community are correct. The door is wide open for further discoveries and, regardless of the final verdict, Kevin will certainly be acknowledged for provoking thought and challenging widely-held opinions.

Likewise, it is not clear what could be the reasons for thermo-chemical piles being stable for 300 Myr and perhaps even longer (Torsvik et al. 2014). In numerical models, it is certainly possible to maintain such piles existing throughout Earth history: Tan et al. (2011) showed that thermo-chemical piles with higher density and bulk modulus than surrounding mantle could survive for billions of years. Mulyukova et al. (2015) showed that even without different bulk modulus, due to mechanical stirring almost neutrally buoyant piles, which hence feature high topography, emerge for a wide range of parameters. With a balance between replenishment (by segregation of oceanic crust material) and destruction (by entrainment in plumes) such piles can survive for billions of years. But in contrast to their stability in time, these piles tend to be mobile in space. Tan et al. (2011) found that a segment of a pile edge can be stationary for 200 million years, while other segments have rapid lateral movement. Also, in the models of Mulyukova et al. (2015) despite prescribed, fixed subduction zone locations, pile shapes are quite variable through time. However, using models of subduction history, it can be shown that piles form at similar locations as the LLSVPs. McNamara and Zhong (2005) found that imposing 119 Myr of subduction history tends to focus dense material into a ridge-like pile beneath Africa and a more rounded pile beneath the Pacific. A time-span of 119 Myr, however, is too short to assess long-term stability in space. Subsequently, using a model of 300 Myr subduction history based on plate reconstructions, Steinberger and Torsvik (2012) found that locations of piles, once they are formed, are quite stable. In particular, if a model is re-initiated from the present-day structure, the pile edges typically move less than 1000 km during 300 Myr of subduction. Bower et al. (2013) used a mantle model setup similar to Tan et al. (2011) but with prescribed surface velocity boundary conditions for the past 250 Myrs, leading to subduction zone locations similar to Steinberger and Torsvik (2012). They found that, with suitable parameters, thermochemical piles remain stable at the core-mantle boundary but deform readily in response to slabs, unless the pile viscosity is 100 times higher than for ambient mantle at the same temperature. Hence, it appears compatible with numerical models that piles have moved little since ~300 Ma. One possible cause would be that they already have been in similar locations as today at 300 Ma, given that subduction zones have probably remained in the same overall regions – mostly away from the piles – since then. It is also possible that the piles, and possible upwellings above them, are themselves controlling the large-scale structure of mantle flow, hence where subduction occurs. One indication is the degree-two structure of plate tectonics, which reveals that underlying mantle upwellings have remained stable for the past 250 Myr in the regions near the two LLSVPs, whereas the regions where most of subduction, and hence most downward flow occurred, have been shifting around, mostly along the great-circle belt between the two LLSVPs (Conrad et al., 2013). Alternatively, or additionally, it may be due to piles being intrinsically more viscous.

Going further back in time, Zhang et al. (2010) used a proxy subduction model (given that exact locations of subduction zones prior to 300 Ma are not well known). They proposed an approximately degree-one initial structure with only one pile beneath Panthalassa (proto-

Pacific basin), because most of the subduction associated with the Pangea assembly occurred in the opposite hemisphere. Subsequently, the structure gradually changes to something closer to “degree two” and more similar to what is observed today, with two separate piles beneath the Pacific and Africa. This result was challenged by Bull et al. (2014), who found that a configuration with only one pile (beneath the Pacific) prior to Pangea assembly, would not evolve to a structure with two piles, even until today. Hence they concluded that a structure similar to the present-day probably existed already at 410 Myr. One reason for this difference is that Bull et al. (2014) used a plate reconstruction, constrained in longitude and corrected for true polar wander, as surface boundary condition, in contrast to the reconstruction of Zhang et al. (2010). The volume of dense material in both studies were similar but Bull et al. (2014) used a ~1% higher density in their models and a slightly lower internal heating within the mantle. The subject was reviewed by Zhong and Liu (2016).

Mantle convection modelling and determination of mineral physics parameters are still at exploratory stages. The potentially very important discovery that the bridgmanite to post-bridgmanite transition in the lower mantle causes a viscosity drop of 3-4 orders of magnitude (Hunt et al. 2009; Ammann et al. 2010) needs to be further explored by experimental and theoretical mineral physics investigations and by convection modelling. Such a viscosity decrease would be most pronounced in the circumpolar high-velocity belt under the Arctic, Asia, Australia, Antarctica and the Americas (Fig. 5). Seismic investigations of D" discontinuities have located the presumed post-bridgmanite transition at 300-400 km and 200-300 km above the CMB under Asia and North to Central America, respectively (e.g. Lay 2015). Such a strong and abrupt viscosity decrease in sinking mantle dominated by cold subducted slab material will ease the flow through the lowermost 300 km and promote the spreading of the material in a relatively thin layer above the CMB (Fig. 6a). This will facilitate efficient heating and partial sinking of dense and thin basaltic crustal slivers (~6.5 km, White and Klein 2014) in the peridotite-dominated flow towards the LLSVP margins. Li et al. (2014) showed that the reduced viscosity allows cold slabs to spread more easily and broadly along the CMB, but that the stability and size of dense reservoirs is not substantially altered by weak post-bridgmanite. Future models should also re-evaluate to what extent slabs are able to trigger plumes along LLSVP margins in the presence of weak post-bridgmanite.

In spite of early interpretations of post-bridgmanite lenses within the NE part of Jason (Lay et al. 2006), recent seismological data from this and other areas are very uncertain. Although a possible combination of high Fe and low Al contents of the LLSVP material might stabilize post-bridgmanite to higher temperatures and lower pressures (Mohn and Trønnes

2015), the strongly positive dp/dT-slope of the post-bridgmanite transition (e.g. Tateno et al. 2009) will generally tend to destabilize the mineral in hot LLSVP material. An absence of post-bridgmanite lenses in the hottest regions of the D" zone, as seems likely at this stage, implies relatively high viscosity (in spite of the high temperature, e.g. Ammann et al. 2010) which would facilitate the stability of LLSVPs.

Compositional asymmetry of plumes and ultra-low velocity zones

The observed semi-parallel “Loa” and “Kea” geochemical trends extending 40-70 km towards NW along the Hawaiian plume track have been noted by several investigators (e.g. Abouchami et al. 2005; Weis 2011). The Kea trend volcanoes with more depleted compositions lie NE of the Loa trend volcanoes, which face the LLSVP interior and are characterized by higher proportions of recycled oceanic crust (ROC). Weis et al. (2011) suggested that the plume zonation could originate by the merging of two lateral D" flows: one towards NE on top of the LLSVP-surface and the other towards SW along the CMB towards the Jason margin. The merging of two lateral flows into the vertical Hawaiian conduit would then result in an asymmetrically zoned plume with the Loa and Kea source materials in the SW and the NE segments of the conduit, respectively. Farnetani and Hofmann (2010; 2012) performed fluid convection modelling of such a divided conduit. Similar chemical plume asymmetry linked to the plume position relative to the nearest LLSVP margin (Fig. 5) has later been documented for Galapagos (Vidito et al., 2013), Samoa (Jackson et al. 2014), Marquesas and Tahiti/Society (Payne et al. 2015) and Tristan (Hoernle 2015).

The double-sided plume-root model (Fig. 6a) implies that a reservoir of ROC forming the upper layer of the LLSVP must be convectively eroded. The ROC stockpile forming the upper LLSVP parts might be continuously replenished in relatively stagnant regions between plumes simultaneously with erosion near plumes rooted along the LLSVP-margins. The average plume spacing along the LLSVP-margin (Fig. 5) is approximately 30°, corresponding to ~1800 km at the CMB. The flow focusing indicated in the figure is unlikely to divide the entire continuous flow front from the circum-polar belt between each of the plumes. Some of the lateral flow towards the LLSVP-margins between two neighbouring plumes is therefore likely to rise onto the LLSVP-surface and be incorporated into the wide and slowly rising mantle column under the residual geoid highs over TUZO and JASON (Fig. 6b). The dense layers and slivers of basaltic composition from the CMB flow have high bulk modulus, due to the presence of β-stishovite ($CaCl_2$-structured silica) and absence of ferropericlase (e.g. Trønnes, 2010; Irifune and Tsuchiya 2015). These ROC slivers may therefore become stagnant in the slowly rising columns of hot mantle above the LLSVPs, and gradually separate and sink to the LLSVP-surface. Such an accumulation may facilitate storage of ROC over time spans of up to about 2.2-2.5 Ga for Samoa, Reunion and parts of the Azores and up to 1.7-2.2 Ga for Iceland, Hawaii and other parts of the Azores (Pb-model ages, Andersen et al. 2015).

The low viscosity associated with post-bridgmanite in the circumpolar belt region and with strongly elevated temperatures next to the core surface and close to the LLSVP-margins will increase the sinking efficiency of folded and disrupted slivers and layers of dense basaltic crust, but will also increase the vigour of convection, counteracting sinking efficiency. A complete separation of basaltic and peridotitic material is therefore unlikely (Li and McNamara 2014). The basaltic layers, constituting 6-7% of subducted slab material, may be folded and stretched during deformation and temporary stagnation in the uppermost lower mantle (e.g. Fukao et al. 2013) and subsequently sinking through the lower mantle, hindering full segregation. The presence of scattered thin (5-50 km thickness) ultra-low velocity zones (ULVZs) preferentially located near the LLSVP margins and in the root zones of plumes originating at the CMB is a key observation (e.g. Thorne and Garnero 2004; Lay 2015). The D" ray coverage required for global mapping the ULVZ distribution is far from complete but combined evidence from several recent studies (e.g. Thorne and Garnero 2004; Thorne et al. 2013; Cottaar and Romanowicz 2012; French and Romanowicz 2015) indicate that ULVZ occurrences are generally correlated with LLSVP margins and the root-zones of deep plumes. Although some suggestions about possible dense and solid ULVZ material have been proposed (Mao et al. 2006; Dobson and Brodholt 2005), seismologists have repeatedly favoured partially molten zones with melt fractions of 15-30%. Several recent studies of high pressure melting relations of peridotitic and basaltic compositions (Andrault et al. 2014; Pradhan et al. 2015) have demonstrated that various basalt solidi are broadly similar to the inferred CMB temperatures of about 3800 K and lower than peridotite solidi of about 4200 K. A strong partitioning of Fe into the partial melts at lowermost mantle conditions (Tateno et al 2014; Pradhan et al. 2015) will make the partially molten regions denser than the surrounding mantle, including the LLSVP material.

In figure 6 we envisage that ULVZs of partially molten basalt may be replenished by partially molten basaltic slivers passing by in the lower part of the lateral flow along the CMB. At the same time, minor amounts of the partially molten ULVZ-material may be entrained into the plume flow in its narrow and fast-flowing root-zone. Based on their seismic tomography observations, French and Romanowicz (2015) suggested the term “necking zone”

for such narrow plume roots. The sinking of partially molten ROC into the ULVZs, followed by re-entrainment of partially molten basalt in the flow on the LLSVP-side, will likely promote the segregation of the basaltic material in the lower part of the flow facing the LLSVP. An additional effect is that the ULVZs may act as long-term reservoirs for ROC material, explaining the old model ages of such plume components (e.g. Andersen et al. 2015)
A relatively strong confinement of ROC to the LLSVP-side of vertically rising plume conduits is expected to diminish as the plume rises through the mantle. Although plume flow is laminar, we expect some folding and deformation on the way towards the surface. The regular compositional asymmetry predicted by the model has been documented only for six of the plumes in figure 5. With further geochemical data collection combined with compilation of existing data, one might find similar asymmetry in other plumes. A number of analytical and numerical models exist for the entrainment of a chemical layer in plumes. The fluid dynamic models of Farnetani and Hofmann (2010) and Farnetani et al. (2012) support the asymmetric entrainment and confinement of ROC slivers on the LLSVP-side of the Hawaiian plume. Sleep (1988) devised a model where a plume rises from a cusp of a thermal boundary layer. Because this model is symmetric, the entrainment of a thin filament of chemically different material occurs in the centre of the plume. Zhong and Hager (2003) formulated a high-resolution numerical model to examine the efficiency of such entrainment, but their model is also axisymmetric. The 2D and 3D numerical models of Jones et al. (2016) yield bilateral asymmetry only for the cases in which the chemical buoyancy is negligible. Otherwise, the dense material is preferentially entrained in the conduit center. Preliminary modelling results by Mulyukova et al. (in preparation) indicate a variety of plumes where ROC – unless it had already been accreted to the LLSVPs – is either well-mixed in the plume or occurs on the side away from the piles, but never only on the side towards the piles. We therefore caution that the scenario sketched in Figure 6 is presently a conceptual idea supported only by some numerical models.

Origin and composition of the LLSVPs

The current resolution of mineral physics data (especially density and bulk and shear moduli) does not allow discrimination between the two commonly invoked alternative LLSVP-materials: basaltic and Fe-rich peridotite. The age and mode of origin of such thermochemical piles, however, can in principle be inferred from an Earth evolutionary and geochemical perspective. Basaltic material accumulation would probably occur over billions of years by separation from subducted lithosphere. In contrast, the emplacement of komatiitic or peridotitic material with elevated Fe/Mg ratios would be confined to Hadean or early Archean, either by the final solidification of a lowermost mantle magma ocean (Labrosse et al 2007; Stixrude et al. 2009) or by sinking of solidified igneous rocks from a melt accumulation zone at 410 km depth (Lee et al. 2010). Some of the recent and most reliable experimental studies have confirmed a strong increase in the Fe/Mg ratio in (residual) melts relative to coexisting bridgmanite, post-bridgmanite and ferropericlase (Tateno et al. 2014; Pradhan et al. 2015). Therefore, the final magma ocean solidification probably involved a separate lower domain of dense residual melts crystallizing from the top to the bottom (Labrosse et al. 2007; Stixrude et al. 2009). Experimental and theoretical investigations by Liebske and Frost (2013) and de Koker et al. (2013) of the MgO-SiO_2 system indicate that residual melts and bulk mantle peridotite have similar (Mg+Fe)/Si ratio. It is therefore likely that the late-stage cumulates will have similar proportions of bridgmanite and (Mg,Fe)O (ferropericlase or magnesiowustite) as the bulk mantle. The oxide proportion of dense primordial cumulates directly above the CMB is expected to decrease by partitioning of the FeO component into the O-undersaturated proto-core (e.g. Frost et al. 2010). The associated increase in bridgmanite/oxide and Mg/Fe ratios would have reduced the density and increased the bulk modulus in the primordial cumulate material. This might have enabled an originally very dense layer covering most of the CMB to segregate into two antipodal thermochemical piles, stabilized near the equator by the Earth's initial fast rotation rate.

Simple dynamic and chemical considerations may indicate composite LLSVPs structures comprising lower parts of primordial Fe-rich peridotites, possibly with bridgmanite/oxide ratio slightly higher than the bulk lower mantle. Accumulations of primordial dense cumulates crystallised in the lowermost mantle or emplaced by sinking from the transition zone (Lee et al. 2010) are unlikely to be stirred into the mantle by convection. By default, it seems inescapable that such material accreted to the LLSVPs during the early history of the Earth. The model ages of the ROC components of various plumes also testify to long-term stockpiles of ROC material in the deep mantle. The inferred lateral D" flow of subducted slab material from the circum-polar belt to the LLSVP margins seem to exclude most of the lowermost mantle as long-term (> 1 Ga) storage sites. In spite of the slowly rising mantle above the LLSVPs, the upper parts of these thermochemical piles seem to be appropriate storage sites (Fig. 6). Because the high bulk modulus of basaltic ROC material results in decreasing density contrast with the ambient peridotitic material with increasing depth, the ROC accumulations will approach neutral buoyancy near the surfaces of the assumed primordial LLSVP piles. The basaltic material might therefore easily become entrained into slowly rising mantle flow and then intermittently sink back against the flow from shallower mantle levels. Such a flow regime might resemble the unstable flow pattern of a “lava lamp”.

Criticism: Statistical attacks

Needless to say, Kevin’s idea that LIPs, kimberlites and hotspots are predominantly sourced by deep mantle plumes from the margins of the LLSVPs (TUZO and JASON) is far from being universally accepted and has generated a vigorous debate in the geophysical literature. Among the most fervent opponents have been the representatives of the Andersonian movement (www.mantleplumes.org; Anderson, 2005; Anderson and King, 2014; Julian et al., 2015), who deny the very existence of deep mantle plumes, and mantle modellers disagreeing with the interpretation of LLSVPs as mantle structures having distinct chemical properties. Several recent papers presented interesting criticism using statistical arguments (Austermann et al., 2014; Davies et al., 2015; Julian et al., 2015).

From the modelling community, Austermann et al. (2014) and Davies et al. (2015) suggested that the observed correlation between the reconstructed LIPs and the margins of TUZO and JASON can be equally well (or even better) explained by deep plumes forming randomly over the entire area associated with the LLSVPs, rather than by plumes from their margins. In other words, the observed pattern, with reconstructed LIPs distributed along the margins and apparently not forming over the interiors of LLSVPs (Fig. 2a), may be just a chance coincidence due to the random process of plume generation. Furthermore, they argued that the two alternatives (plumes from the entire LLSVPs and plumes from the margins) could not be distinguished based on a statistical analysis of the observed distribution of LIPs. This criticism was addressed in the study of Doubrovine et al. (2016), in which they used a nonparametric approach based on empirical distribution function (EDF) statistics to test the spatial LIP distribution. That study showed that although the hypothesis proposing that LIP-sourcing plumes form randomly over the entire area of the slower-than-average shear-wave velocities associated with TUZO and JASON cannot be ruled out completely, the probability models assuming that plumes rise from the LLSVP margins, provide a much better fit to the LIP data. Hence, we consider it reasonable to prefer the latter hypothesis.

An example from the Andersonian movement includes the study of Julian et al. (2015) who suggested that the “The supposed LIP-Hotspot-LLSVP correlations probably are examples of the Hindsight Heresy”, by which they meant restricting statistical tests to the data that have been initially used to formulate the hypothesis being tested. This accusation is not appropriate. The first paper talking about correlation between hotspots and deep mantle lateral shear-wave velocity gradients (mainly along the LLSVP margins) was by Thorne et al. (2004). But since it was not clear which hotspots were sourced by deep mantle plumes, Torsvik et al. (2006) used reconstructed LIPs, which is not the same data sample as in Thorne et al. (2004). A statistical test of the correlation between the LIPs and LLSVPs was first undertaken by Burke et al. (2008); more recent studies include Austermann et al. (2014), Davies et al. (2015) and Doubrovine et al. (2016). Torsvik et al. (2010) performed a statistical analysis for the distribution of kimberlites, which is yet another data set. In contrast, the distribution of hotspots has not been the subject of statistical tests in the work of Kevin and his collaborators because it is unclear which hotspots are sourced by deep mantle plumes as mentioned above.

The study of Julian et al. (2015) focused entirely on the analysis of the distribution of present hotspots, criticizing some technical aspects of the statistical approach used by Burke et al. (2008), which according to Julian et al. (2015) led to “inadvertent hindsight effects” in estimating the significance of the correlation between the LIPs and LLSVPs. Ironically, even after “correcting” for these effects, they arrived at the conclusion that there is a very strong correlation (99% confidence level) between the hotspots and the margins of LLSVPs. Thus, regardless of the discussion on whether Burke et al. (2008) overestimated the confidence levels in their analysis (which is beyond the scope of this paper), the correlation is real and cannot be attributed to the heretical thinking of some of the involved parties. The same is true for the correlations involving LIPs and kimberlites as was repeatedly shown by, for example, Torsvik et al. (2010), Austermann et al. (2014) and Doubrovine et al. (2016). Since we have clearly identified the mechanism for causation – i.e. our hypothesis that plumes rising from the margins of TUZO and JASON lead to the observed correlation – we consider this criticism unfounded.

Julian et al. (2015) used five catalogues of hotspots compiled by different authors, with 37 to 72 hotspots in each catalogue. These catalogues are not independent from each other, but more importantly, it has been long suspected that many of hotspots included in these lists (the majority in fact) may not have deep plume origin. For instance, Ritsema and Allen (2003) concluded that only eight hotspots had a possible deep plume origin, based on underlying low shear-wave-velocities in both the upper and lower mantle. With other criteria, including the presence or not of a volcanic track and a starting LIP, high $^{3}He/^{4}He$ and tomographic evidence, Courtillot et al. (2003) considered seven out of 49 hotspots (only 14%)

originate from the deep mantle. We note that all these “primary” hotspots (Afar, Easter, Iceland, Hawaii, Louisville, Reunion and Tristan) are located above or near the edges of TUZO and JASON (Fig. 7c). Courtillot et al. (2003) also distinguished between “secondary” plumes — originating from the base of the transition zone on the tops of TUZO and JASON (Fig. 4a) — and a third type of superficial “Andersonian” hotspots linked to lithosphere tensile stresses and decompression melting. Montelli et al. (2006) identified 12 hotspots of possible deep origin from seismic tomography. In a more recent study, French and Romanowicz (2015) identified 20 primary or clearly resolved plumes in the Earth’s mantle (Fig. 7c). They also included a third category (“Somewhat resolved”) of seven hotspots.

A simple visual comparison of the position of the 20 primary and clearly resolved hotspots of French and Romanowicz (2015) with the tomography (Fig. 7c) suggests that most of them are located near the margins of TUZO and JASON. The exceptions are the Samoa, Tahiti and Caroline hotspots, which are located closer to the centre of JASON (see also Fig. 5). It is also noteworthy that all hotspots (except Louisville) that are commonly used for plate reconstructions in a hotspot reference frame, i.e. Hawaii, New England, Reunion and Tristan (Fig. 7c), lie directly above the margins of TUZO and JASON, and not above their centres. The pattern of hotspots is quite similar to that for reconstructed LIPs (except Columbia River Basalt, 15 Ma) since the Cretaceous (Fig. 7d). However, unlike LIPs, some hotspot locations tend to be displaced from the PGZ contours toward the interiors of the LLSVPs, which is most clear for the Pacific hotspots.

The Burkian Earth

While physicists are fantasizing about a unified theory that can explain just about everything from the subatomic particles (quantum mechanics) to the origin of the Universe (general relativity), Darwin (1858) explained nearly all about life on Earth with one unified vision (Livio 2013). In Earth Sciences the description of the movement and deformation of the Earth's outer layer has evolved from Continental Drift (1912) into Sea-Floor Spreading (1962) and then to the paradigm of Plate Tectonics in the mid to late 1960s. Plate Tectonics is as fundamentally unifying to the Earth Sciences as Darwin's Theory of Evolution is to Life Sciences, but it is an incomplete theory without a clear understanding of how plate tectonics and mantle plumes interact, a problem that Kevin set out to resolve more than a decade ago by proposing a simple conceptual model, which we will refer to as “the Burkian Earth”.

The Burkian Earth is a simple and stable degree-2 planet (Fig. 4c). TUZO and JASON are thermochemical reservoirs, probably both denser and hotter in the lowermost parts. The Burkian Earth is dominated by small-scale convection in the upper mantle and circulation in the lower mantle, which is mostly restricted to sinking slabs and rising thermochemical plumes and at most sluggish elsewhere. Subduction zones show a predominantly large-scale pattern, especially the "ring of fire" circling the entire Pacific. Therefore slabs sinking all the way to the lowermost mantle also relate to long-wavelength lower mantle structure dominated by degree 2. Plumes ~~are~~ rise vertically (no advection as modelled in Fig. 7c) from the margins of TUZO and JASON — the plume generation zones — which Kevin would describe as loci of an intermittent or continuous upward flux of hot and buoyant material from the CMB. On the surface, this flux is witnessed by the catastrophic emplacement of LIPs and less energetic kimberlites and hotspot volcanoes, of which a few lie on tracks departing from LIPs.

On Kevin's planet, all LIPs and kimberlites are sourced by plumes from the plume generation zones at the CMB, but based on global tomography models there are exceptions such as the 15 Myr Columbia River Basalt and Cretaceous-Tertiary kimberlites in NW America. Additionally, no hotspots in this region or in nearby offshore areas (e.g., Yellowstone, Raton, Bowie and Cobb hotspots in Fig. 7c) have been classified as deep plumes. There are, however, published S-SKS models (Castle et al. 2000; Kuo et al. 2000) that do show low velocity areas at the CMB beneath the Columbia River Basalts and surrounding areas, and also in some other regions, such that with the choice of particular tomography models, many more plumes can be fitted nearly vertically above a PGZ. However, those features do not show up in some other tomography models. French and Romanowicz (2015) do not image low-velocity regions at the CMB vertically below Yellowstone, although they do see a small low-velocity region (Fig. 7a) approximately centred beneath Las Vegas, about 1000 km towards the southwest. Schmandt et al. (2012) find an upward deflection of the 660-km discontinuity beneath Yellowstone and low seismic velocities in the mantle between 660 and ~900 km depth, displaced about 200 km to the southwest, both suggesting a lower-mantle origin of the Yellowstone plume. Their results give no hint of a plume conduit at greater depth, but numerical models of plumes deflected in large-scale mantle flow predict that a plume source in the lowermost mantle should be displaced about 500-1000 km to the southwest (Steinberger, 2000) in a similar region to where French and Romanowicz (2015) image low seismic velocities.

The Burkian Earth is very different from the "Andersonian" Earth (Fig. 4b) where slabs are often halted by the 660-km discontinuity and only punch through after sufficient accumulation, whereas plumes do not exist and hotspot volcanism is only linked to lithosphere tensile stresses, cracking and decompression melting. Whole mantle tomography (Fig. 7a, b), the similarity between reconstructions based on hotspot locations and palaeomagnetism, and the locations of LIPs and kimberlites in relation to the tomography of the lowermost mantle (TUZO and JASON) are clearly at odds with such a planet. Many hotspots, however, could be of the Andersonian type. Interestingly, the Andersonian Earth includes ancient low velocity regions in the deepest mantle (Fig. 4b), which are comparable with TUZO and JASON. On the Burkian Earth these are primordial thermochemical piles that possibly formed during early magma ocean crystallization (or shortly afterward), perhaps by magmatic segregations of Fe-rich peridotitic or komatiitic materials.

It is still unclear, though, why lower mantle structures similar to today would already have existed back in the Hadean. If, as envisioned by Kevin, only slabs are going down and plumes are coming up — and nothing else moves — it may be easier to also keep piles stable where they are. But even in this case, piles might be disrupted if subduction occurs directly above them. So is it possible that piles survive that? Or is there a mechanism to keep subduction zones away from piles? Could large-scale upwellings act as “mantle anchor structure” (Dziewonski et al. 2010) that also controls where downward flow and subduction occurs? An indication of that could be the net characteristics of plate tectonics, which reveal that active mantle upwellings have been stable since 250 Ma, whereas the regions where most subduction occurs have been more mobile (Conrad et al., 2013). Or could it be that subduction keeps itself in place (Baes and Sobolev 2014)? All these are open questions, and at the moment we don't even know with certainty whether thermochemical piles were spatially stable for much longer than 300 Myr – we can only say that their stability is consistent with data, but it is not necessarily required, due to uncertainties in longitude of continents (Torsvik et al. 2014). Kevin's provoking ideas have clearly been, and will continue to be, a source of inspiration for the studies that shed light on these questions.

Acknowledgements

This paper is dedicated to Kevin Burke for his long-life service to science, and as an inspiratory mentor and debater. Trond Torsvik also acknowledges John Dewey and colleagues at the University of Oxford for stimulating years during his first position there in the 1980’s. The Research Council of Norway through its Centres of Excellence funding scheme, project number 223272 (CEED) and the European Research Council under the European Union's Seventh

Framework Programme (FP7/2007-2013)/ERC Advanced Grant Agreement Number 267631 (Beyond Plate Tectonics) are acknowledged for financial support. We thank three anonymous reviewers for useful suggestions.

References

Abouchami, W., Galer, S.J.G., and Hofmann, A.W. 2000. High precision lead isotope systematics of lavas from the Hawaiian Scientific Drilling Project. Chemical Geology, **169**: 187–209.

Ammann M.W., Brodholt J.P., Wookey J., and Dobson D.P. 2010. First-principles constraints on diffusion in lower-mantle minerals and a weak D" layer. Nature, **465**: 462–465.

Andrault, D., Pesce, G., Bouhifd, M.A., Bolfan-Casanova, N., Hénot, J.-M., and Mezouar, M. 2014. Melting of subducted basalt at the core-mantle boundary. Science, **344**: 892–895.

Andersen, M.B., Elliott, T., Freymuth, H., Sims, K.W.W., Niu, Y., and Kelley, K.A. 2015. The terrestrial uranium isotope cycle. Nature, **517**: 356–359.

Anderson, D.L. 2005, Scoring hotspots: The plume and plate paradigms, *In* Plates, plumes, and paradigms. Edited by G.R. Foulger, J.H. Natland, D.C. Presnall and D.L. Anderson, Geological Society of America Special Paper 388, pp. 31–54, doi: 10.1130/2005.2388(04).

Anderson, D.L., and King, S.D. 2014. Driving the Earth machine? Science, **346**: 1184–1185.

Austermann, J., Kaye, B.T., Mitrovica, J.X., and Huybers, P. 2014. A statistical analysis of the correlation between Large Igneous Provinces and lower mantle seismic structure. Geophysical Journal International, **197**: 1–9.

Baes, M., and Sobolev, S. 2014. Subduction initiation triggered by mantle suction flow. Geophysical Research Abstracts, **16**: EGU2014-6831.

Becker, T.W., and Boschi, L. 2002. A comparison of tomographic and geodynamic mantle models. Geochemistry Geophysics Geosystems, **3**: 1003, doi:10.1029/2001GC000168.

Bower, D.J., Gurnis, M., and Seton, M. 2013. Lower mantle structure from paleogeographically constrained dynamic Earth models. Geochemistry Geophysics Geosystems, **14**: 44–63, doi:10.1029/2012GC004267.

Bull, A.L., Domeier, M., and Torsvik, T.H. 2014. The effect of plate motion history on the longevity of deep mantle heterogeneities. Earth and Planetary Science Letters **40**: 172–182.

Burke, K. 2011. Plate Tectonics, the Wilson Cycle, and Mantle Plumes: Geodynamics from the Top. Annual Reviews of Earth and Planetary Sciences, **39**: 1–29.

Burke, K., and Wilson, J.T. 1972. Is the African plate stationary? Nature, **239**: 387–390.

Burke, K., and Dewey, J.F. 1973. Plume generated triple junctions: Key indicators in applying plate tectonics to old rocks. The Journal of Geology, **81**: 406-433.

Burke, K., Kidd, W.S.F., and Wilson, J.T. 1973a. Plumes and concentric plume traces of the Eurasian plate. Nature, **241**: 128–129.

Burke, K., Kidd, W.S.F., and Wilson, J.T. 1973b. Relative and latitudinal motion of Atlantic hot spots. Nature, **245**: 133–137.

Burke, K., and Wilson, J.T. 1976. Hot spots on the earth’s surface. Scientific American, **235** (2): 46–60.

Burke, K., and Torsvik, T.H. 2004. Derivation of large igneous provinces of the past 200 million years from long-term heterogeneities in the deep mantle. Earth and Planetary Science Letters, **227**: 531–538.

Burke, K., Steinberger, B., Torsvik, T.H., and Smethurst, M.A. 2008. Plume Generation Zones at the margins of Large Low Shear Velocity Provinces on the Core-Mantle Boundary. Earth and Planetary Science Letters, **265**: 49–60.

Castle, J.C., Creager, K.C., Winchester, J.P., and van der Hilst, R.D. 2000. Shear wave speeds at the base of the mantle. Journal of Geophysical Research, **105**: 21,543–21,558.

Chandler, M. T., Wessel, P., Taylor, B., Seton, M., Kim, S.-S., and Hyeong, K. 2012. Reconstructing Ontong Java Nui: Implications for Pacific absolute plate motion, hot spot drift and true polar wander. Earth and Planetary Sciencs Letters, **331-332**: 140–151. doi:10.1016/j.epsl.2012.03.017.

Cottaar, S., and Romanowicz, B. 2012. An unusually large ULVZ at the base of the mantle near Hawaii. Earth and Planetary Science Letters, **355–356**: 213–222.

Courtillot, V., Davaille, A., Besse, J., and Stock, J. 2003. Three distinct types of hotspots in the Earth’s mantle. Earth and Planetary Science Letters, **205**: 295–308.

Davies, D.R., Goes, S., and Sambridge, M. 2015. On the relationship between volcanic hotspot locations, the eruption sites of large igneous provinces and deep seismic structure. Earth and Planetary Science Letters, **411**: 121–130.

Darwin, C.R. 1859. On the origin of species by means of natural selection, or the preservation of favoured races in the struggle for life. John Murray, London.

de Koker, N.B., Karki, B., and Stixrude, L.N. 2013. Thermodynamics of the MgO-SiO_2 liquid system in Earth’s lowermost mantle from first principles. Earth and Planetary Science Letters, **361**: 58-–63.

Dewey, J.F., and Burke, K. 1973. Tibetan, Variscan and Precambrian basement reactivation: products of continental collision. The Journal of Geology, **81**: 683-692

Dobson, D.P., and Brodholt, J.P. 2005. Subducted banded iron formations as a source of ultralow-velocity zones at the core-mantle boundary. Nature, **434**: 371–374.

Doubrovine, P.V., Steinberger, B., and Torsvik, T.H. 2012. Absolute plate motions in a reference frame defined by moving hotspots in the Pacific, Atlantic and Indian oceans. Journal of Geophysical Research*,* **117**: B09101. doi:10.1029/2011JB009072.

Doubrovine, P.V., Steinberger, B., and Torsvik, T.H. 2016. A failure to reject: Testing the correlation between large igneous provinces and deep mantle structures with EDF statistics. Geochemistry Geophysics Geosystems, in revision.

Dziewonski, A.M., Lekic, V. and Romanowicz, B.A. 2010. Mantle anchor structure: An argument for bottom up tectonics. Earth and Planetary Science Letters, **299**: 69-–79.

Eldholm, O., and Coffin, M.F. 2000. Large Igneous Provinces and Plate Tectonics. *In* The History and Dynamics of Global Plate Motions. Edited by M.A. Richards, R.G. Gordon and R.D. van der Hilst. American Geophysical Union Monograph 121, Washington DC., pp. 309–326

Farnetani, C.G., and Hofmann, A.W. 2010. Dynamics and internal structure of the Hawaiian plume. Earth and Planetary Science Letters, **295**: 231–240.

Farnetani, C.G., Hofmann, A.W., and Class, C. 2012. How double volcanic chains sample geochemical anomalies from the lowermost mantle. Earth and Planetary Science Letters, **359-360**: 240–247.

Ford, H.A., Long, M.D., He, X., and Lynner, C. 2015. Lowermost mantle flow at the eastern edge of the African Large Low Shear Velocity Province. Earth and Planetary Science Letters, **420**: 12–22.

French, S.W., and Romanowicz, B. 2015. Broad plumes rooted at the base of the Earth's mantle beneath major hotspots. Nature, **525**: 95–99.

Frost, D.J., Asahara, Y., Rubie, D.C., Miyajima, N., Dubrovinsky, L.S., Holzapfel, C., Ohtani, E., Miyahara, M., and Sakai, T. 2010. Partitioning of oxygen between the Earth's mantle and core. Journal of Geophysical Research, **115**: B02202. doi:10.1029/2009JB006302.

Garnero, E.J., Lay, T., and McNamara, A. 2007. Implications of lower mantle structural heterogeneity for existence and nature of whole mantle plumes. Geological Society of America Special Paper, **430**, 79–102.

Gaßmöller, R., 2014. The interaction of subducted slabs and plume generation zones in geodynamic models. Ph.D. thesis, University of Potsdam.

Girard, J., Amulele, G., Farla, R., Mohiuddin, A., and Karato, S.-I. 2016. Shear deformation of bridgmanite and magnesiowüstite aggregates at lower mantle conditions. Science, **351**: 144–147.

Hager, B.H., and Richards, M.A. 1989. Long-wavelength variations in Earth's geoid: Physical models and dynamical implications. Philosophical Transactions of the Royal Society London, Series A, **328**: 309–327.

Hassan, R., Flament, N., Gurnis, M., Bower, D.J., and Müller, D. 2015. Provenance of plumes in global convection models. Geochemistry Geophysics Geosystems, **16**: 1465–1489. doi:10.1002/2015GC005751.

Heaman, L.M., Pell. J., Grutter, H.S., and Creaser, R.A. 2015. U–Pb geochronology and Sr/Nd isotope compositions of groundmass perovskite from the newly discovered Jurassic Chidliak kimberlite field, Baffin Island, Canada. Earth and Planetary Science Letters, **415**: 183–199.

Hoernle, K., Rohde, J., Hauff, F., Garbe-Schönberg, D., Homringhausen, S., Werner, R., and Morgan, J.P. 2015. How and when plume zonation appeared during the 132 Myr evolution of the Tristan Hotspot. Nature Communications, **6**: 7799. doi:10.1038/ncomms8799.

Hunt S.A., Weidner D.J., Li L., Wang, L., Walte, N.P., Brodholt, J.P., and Dobson, D.P. 2009. Weakening of calcium iridate during its transformation from perovskite to post-perovskite. Nature Geosciences, **2**: 794–797.

Irifune, T., and Tsuchiya, T. 2015. Phase Transitions and Mineralogy of the Lower Mantle. Treatise on Geophysics, Second edition, 2-03: 33–60.

Jackson, M.G., Hart, S.R, Konter, J.G., Kurz, M.D., Blusztajn, J., and Farley, K.A. 2014. Helium and lead isotopes reveal the geochemical geometry of the Samoan plume. Nature, **514**: 355–358.

Jones T.D., Davies, D.R., Campbell, I.H., Wilson, C.R., and Kramer, S.C., 2016. Do mantle plumes preserve the heterogeneous structure of their deep-mantle source? Earth and Planetary Science Letters, **434**: 10–17. doi:10.1016/j.epsl.2015.11.016.

Julian, B., Foulger, G., Hatfield, O., Jackson, S., Simpson, E., Einbeck, J., and Moore, A. 2014. Hotspots in Hindsight. The Geological Society of America Special Paper 514, 105–121.

Karato, S.-I., and Li, P. 1992. Diffusion creep in perovskite: Implications for the rheology of the lower mantle. Science, **255**: 1238–1240.

Kuo, B.Y., Garnero, E.J., and Lay, T. 2000. Tomographic inversion of S-SKS times for shear velocity heterogeneity in D’’: degree 12 and hybrid models. Journal of Geophysical Research, **105**: 28,139–28,157.

Labrosse, S., Hernlund, J.W., and Coltice, N. 2007. A crystallizing dense magma ocean at the base of the Earth’s mantle. Nature, **450**: 866–869.

Lay T. 2015. Deep Earth Structure – Lower Mantle and D". Treatise on Geophysics, Second edition, 1-24: 683–723.

Lay T., Hernlund J., Garnero E.J., and Thorne M.S. 2006. A post-perovskite lens and D" heat flux beneath the central Pacific. Science, **314**: 1272–1276.

Lee, C.-T.A., Luffi, P., Hoink, T., Li, J., Dasgupta, R., and Hernlund, J. 2010. Upside-down differentiation and generation of a ‘primordial’ lower mantle. Nature, **463**: 930–933.

Lekic V., Cottar S., Dziewonski A., and Romanowicz B. 2012. Cluster analysis of global lower mantle tomography: A new class of structure and implications for chemical heterogeneity. Earth and Planetary Science Letters, **357**: 68–77.

Liebske, C., and Frost, D.J. 2012. Melting phase relations in the MgO–$MgSiO_3$ system between 16 and 26 GPa: Implications for melting in Earth’s deep interior. Earth and Planetary Science Letters, **345-348**, 159–170.

Li, X.D., and Romanowicz, B. 1996. Global mantle shear-velocity model developed using nonlinear asymptotic coupling theory. Journal of Geophysical Research, **101**: 22,245–22,272.

Li, M., and McNamara, A.K. 2013. The difficulty for subducted oceanic crust to accumulate at the Earth’s core-mantle boundary. Journal of Geophysical Research, **118**: 1807–1816.

Li, Y., Deschamps, F., and Tackley, P.J. 2014. Effects of low-viscosity post-perovskite on the stability and structure of primordial reservoirs in the lower mantle. Geophysical Research Letters, **41**: 7089–7097.

Livio, M. 2013. Brilliant blunders: From Darwin to Einstein — Colossal mistakes by great scientists that changed our understanding of life and the universe. Simon & Schuster, New York.

Long, M.D., and Lynner, C. 2015. Seismic anisotropy in the lowermost mantle near the Perm Anomaly. Geophysical Research Letters, **42**: 7073–7080. doi:10.1002/2015GL065506.

Mao, W.L., Mao, H.-K., Sturhahn, W., Zhao, J., Prapenka, V.B., Meng, Y., Shu, J., Fei, Y., and Hemley, R.J. 2006. Iron-rich post-perovskite and the origin of ultralow-velocity zones. Science, **312**: 564–565.

McNamara, A.K., and Zhong, S.J. 2005.Thermochemical structures beneath Africa and the Pacific Ocean. Nature, **437**: 1136–1139.

Mohn, C.E., and Trønnes, R.G. 2015. Partitioning of $FeSiO_3$ and $FeAlO_3$, Fe-spin state and elasticity for bridgmanite and post-bridgmanite. Goldschmidt Abstracts, **215**: 2163.

Montelli, R., Nolet, G., Dahlen, F., and Masters, G. 2006. A catalogue of deep mantle plumes: new results from finite-frequency tomography. Geochemistry Geophysics Geosystems, **7**: Q11007. doi:10.1029/2006GC001248.

Morgan, W.J. 1971. Convection plumes in the lower mantle. Nature **230**: 42–43.

Mulyukova, E., Steinberger, B., Dabrowski, M., and Sobolev, S.V. 2015. Survival of LLSVPs for billions of years in a vigorously convecting mantle: replenishment and destruction of chemical anomaly. Journal of Geophysical Research, **120**, 3824–3847. doi:10.1002/2014JB011688.

Mulyukova, E., Steinberger, B., Dabrowski, M., and Sobolev, S.V. Residence time of segregated oceanic crust in the deep mantle. In preparation.

Olierook, H.K.H., Merle, R.E., Jourdan, F., Sircombe, K., Fraser, K., Timms, N.E., Nelson, G., Dadd, K.A., Kellerson, L., and Borissova, I. 2015. Age and geochemistry of magmatism of the oceanic Wallaby Plateau and implications for the opening of the Indian Ocean. Geology, **43**: 971–974.

Payne, J.A., Jackson, M.G., and Hall, P.S. 2015. Parallel volcano trends and geochemical asymmetry of the Society Islands hotspot track. Geology, **41**: 19–22.

Pradhan,G.K., Fiquet, G., Siebert, J., Auzende, A.-L., Morard, G., Antonangeli, D., and Garbarino, G. 2015. Melting of MORB at core-mantle boundary. Earth and Planetary Science Letters, **431**: 247251.

Ritsema, J., and Allen, R.M. 2003. The elusive mantle plume. Earth and Planetary Science Letters, **207**: 1–12.

Schmandt, B., Dueker, K., Humphreys, E., and Hansen, S. 2012. Hot mantle upwelling across the 660 beneath Yellowstone. Earth and Planetary Science Letters, **331–332**: 224–236.

Scotese, C.R., Gahagan, L.M., and Ross, M.R. 1987. Phanerozoic Plate Tectonic Reconstructions. Tech, Rep. No. **90**, Inst. Geophysics, Univ. Texas, Austin.

Sleep, N.H. 1988. Gradual entrainment of a chemical layer at the base of the mantle by overlying convection. Geophysical Journal, **95**: 437–447. doi:10.1111/j.1365-246X.1988.tb06695.x.

Solomatov, V.S., and Reese, C.C. 2008. Grain size variations in the Earth's mantle and the evolution of primordial chemical heterogeneities. Journal Geophysical Research, **113**: B07408. doi:10.1029/2007JB005319.

Steinberger, B. 2000. Plumes in a convecting mantle: Models and observations for individual hotspots. Journal of Geophysical Research, **105**: 11,127–11,152.

Steinberger, B., and O'Connell. R.J. 1998. Advection of plumes in mantle flow; implications on hotspot motion, mantle viscosity and plume distribution. Geophysical Journal International, **132**: 412–434.

Steinberger, B., and Torsvik, T.H. 2008. Absolute plate motions and true polar wander in the absence of hotspot tracks. Nature, **452**: 620–623.

Steinberger, B., and Torsvik, T.H. 2012. A geodynamic models of plumes from the margins of Large Low Shear Velocity Provinces. Geochemistry Geophysics Geosystems, **13**: Q01W09. doi:10.1029/2011GC003808.

Steinberger, B., Sutherland, R., and O'Connell, R.J., 2004. Prediction of Emperor-Hawaii seamount locations from a revised model of plate motion and mantle flow. Nature, **430**, 167–173.

Stixrude, L., de Koker, N., Sun, N., Mookherjee, M., and Karki, B. 2009. Thermodynamics of silicate liquids in the deep Earth. Earth and Planetary Science Letters, **278**: 226–232.

Tan, E., and Gurnis, M. 2005. Metastable superplumes and mantle compressibility: Geophysical Research Letters, **32**: L20307. doi:10.1029/2005GL024190.

Tan, E., Leng, W., Zhong, S., and Gurnis, M. 2011. On the location of plumes and lateral movement of thermochemical structures with high bulk modulus in the 3-D compressible mantle. Geochemistry Geophysics Geosystems, **12**, Q07005. doi:10.1029/2011GC003665.

Tateno, S., Hirose, K., Sata, N., and Ohishi, Y. 2009. Determination of post-perovskite phase transition boundary up to 4400 K and implications for thermal structure in D″ layer. Earth and Planetary Science Letters, **357**: 68–77.

Tateno, S., Hirose, K., and Ohishi, Y. 2014. Melting experiments on peridotite to lowermost mantle conditions. Journal of Geophysical Research, **119**: 4684–4694.

Thorne, M.S., and Garnero E.J. 2004. Inferences on ultralow-velocity zone structure from a global analysis of SPdKS waves. Journal of Geophysical Research, **109**: B08301. doi:10.1029/2004JB003010.

Thorne, M.S., Garnero, E.J., and Grand, S. 2004. Geographic correlation between hot spots and deep mantle lateral shear-wave velocity gradients. Physics of the Earth and Planetary Interiors, **146**, 47–63.

Thorne M.S., Garnero E.J., Jahnke G., Igel H., and McNamara, A.K. 2013. Mega ultra low velocity zone and mantle flow. Earth and Planetary Science Letters, **364**: 59–67.

Torsvik, T.H., Smethurst, M.A., Burke, K., and Steinberger, B. 2006. Large Igneous Provinces generated from the margins of the Large Low Velocity Provinces in the deep mantle. Geophysical Journal International, **167**: 1447–1460.

Torsvik, T.H., Müller, R.D., Van der Voo, R., Steinberger, B., and Gaina, C. 2008a. Global Plate Motion Frames: Toward a unified model. Reviews of Geophysics, **46**, RG3004. doi:10.1029/2007RG000227.

Torsvik, T.H., Smethurst, M.A., Burke, K., and Steinberger, B. 2008b. Long term stability in Deep Mantle structure: Evidence from the ca. 300 Ma Skagerrak-Centered Large Igneous Province (the SCLIP). Earth Planetary Science Letters, **267**:, 444–452.

Torsvik, T.H. Burke, K., Steinberger, B., Webb, S.C., and Ashwal, L.D. 2010. Diamonds sourced by plumes from the core mantle boundary. Nature, **466**: 352–355.

Torsvik, T.H., Van der Voo, R., Doubrovine, P.V., Burke, K., Steinberger, B., Ashwal, L.D., Trønnes, R., Webb, S.J., and Bull, A.L. 2014. Deep mantle structure as a reference frame for movements in and on the Earth. Proceedings of the National Academy of Sciences, **111**: 24, 8735–8740

Trønnes, R.G. 2010. Structure, mineralogy and dynamics of the lowermost mantle. Mineralogy and Petrology, **99**: 243–261.

Vidito, C., Herzberg, C., Gazel, E., and Harpp, K. 2013. Lithological structure of the Galápagos Plume. Geochemistry, Geophysics, Geosystems, **14**: 4214–4240.

Weis, D., Garcia, M.O., Rhodes, J.M., Jellinek, M., and Scoates, J.S. 2011. Role of the deep mantle in generating the compositional asymmetry of the Hawaiian mantle plume. Nature Geoscience, **4**: 831–838.

White W.M., and Klein, E.M. 2014. Composition of the oceanic crust. *In* Treatise on Geochemistry, Second Edition, 4-13: 457–496.

Wilson, J.T. 1963. A possible origin of the Hawaiian islands. Canadian Journal of Physics, **41**: 863–870.

Wilson, J.T. 1966. Did the Atlantic close and then re-open? Nature, **211**: 676–681.

Wilson, J.T., and Burke, K. 1972. Two types of mountain building. Nature, **239**: 448–449.

Zhang, N., Zhong, S.J., Leng, W., and Li, Z.X. 2010. A model for the evolution of the Earth's mantle structure since the Early Paleozoic. Journal of Geophysical Research, **115**: B06401. doi:10.1029/2009JB006896.

Zhong, S., and Liu, X. 2016. The long-wavelength mantle structure and dynamics and implications for large-scale tectonics and volcanism in the Phanerozoic. Gondwana Research, **29**: 83-–104.

Zhong, S., and Hager, B.H. 2003. Entrainment of a dense layer by thermal plumes. Geophysical Journal International, **154**: 666–676. doi:10.1046/j.1365-246X.2003.01988.x.

Zurevinski, S.E., Heaman, L.M., and Creaser, R.A. 2011. The origin of Triassic/Jurassic kimberlite magmatism, Canada: Two mantle sources revealed from the Sr-Nd isotopic composition of groundmass perovskite. Geochemistry, Geophysics, Geosystems, **12**: Q09005, doi:10.1029/2011GC003659.

Zhong, S.J., Zuber, M.T., Moresi, L., and Gurnis, M. 2000. Role of temperature-dependent viscosity and surface plates in spherical shell models of mantle convection. Journal of Geophysical Research, **105**: 11063–11082.

FIGURE CAPTIONS

Figure 1 (a) First published paper of reconstructed LIPs (201–15 Ma; Burke and Torsvik 2004) draped on the SMEAN shear-wave tomography model of Becker and Boschi (2002). Reconstructed LIPs plot within — or overlay the edges — of low-velocity regions of the D" zone. The Columbia River (CR, 15 Ma), Maud Ridge (MR. assigned 73 Ma in this paper but now assigned an age of 125 Ma) and Manihiki Plateau (MP, 123 Ma) are exceptions in this diagram. The oldest reconstructed LIP in this diagram was the 201 Ma Central Atlantic Igneous Province (marked C). (b) Follow-up LIP reconstructions by Torsvik et al. (2006) with revised age for Maud Ridge (MR, 125 Ma) and extended back to 251 Ma (Siberian Traps, ST). In this paper the steepest gradients in the SMEAN tomography model were around the 1% slow contour (red thick line) and dubbed FSB (faster/slower boundary). (a, b) are two different but closely similar palaeomagnetic reconstructions but in (c) we show the first LIP reconstructions using a hybrid mantle frame (Torsvik et al. 2010; see text), and extended back to eruption of the Skagerrak Centred LIP (SC). The 1% slow in (b) was dubbed the PGZ (plume generation zone) from 2008 and onwards (Burke et al. 2008).

Figure 2 (a) Up-to date reconstruction of all Phanerozoic LIPs (15-510 Ma) using a hybrid reference frame (updated from Fig. 1c) and draped on the s10mean tomographic model of Doubrovine et al. (2016). The plume generation zone (PGZ) in this model corresponds to the 0.9% slow contour. LIPs with red-squared symbols are reconstructed with moving and fixed hotspot reference frames whilst those with green-squared symbols use a true polar wander corrected reference frame/plume generation zone method (see text). LIP numbers (ages in Ma) are as follows: 15 (Columbia River), 31 (East African), 62 (North Atlantic Igneous Province), 65(Deccan), 73 (S. Leone Rise), 87 (Madagascar), 95 (Broken Ridge), 99 (Hess Ridge), 100 (Central Kerguelen), 100 (Agulhas Plateau), 111 (Nauru), 114 (South Kerguelen), 118 (Rajhmahal), 123 (Ontong Java Nui), 124 (Wallaby Plateau), 125 (Maud Rise), 132 (Bunbury), 134 (Parana-Etendeka), 136 (Gascoyne), 145 (Magellan Rise), 147 (Shatsky Rise), 155 (Argo Margin), 182 (Karroo), 200 (Central Atlantic Magmatic Province), 251 (Siberian Traps), 260 (Emeishan), 285(Panjal Traps/Tethyan Plume), 297 (Skagerrak Centred LIP, SCLIP), 360 (Yakutsk), 400 (Altay-Sayan), 510 (Kalkarindji). (b) 1773 Phanerozoic kimberlites reconstructed as for the LIPs in (a) but here draped on seismic voting-map contours in the lower mantle (Lekic et al., 2012). In this model five contours (only three shown on diagram) define the LLSVPs and count 0 (blue) denotes faster regions in the lower mantle. Note that this seismic map is derived from cluster analysis between 1000 and 2800 km depth; similarity of the maps in (a) and (b) therefore suggests that most of the lower mantle above the LLSVPs is warmer than the average mantle. The s10mean zero contour in (a) is shown for comparison (white lines). Blue kimberlite symbols are those that are anomalous by overlying the faster regions of the lower mantle.

Figure 3 Examples of global plate reconstructions (same reference frame as in Fig. 2) and the distribution of kimberlites (stars) and LIPs (squares). Kimberlites with blue-coloured stars are somewhat anomalous. LIPs number are ages in million years and acronyms are as follows: A, Argo Plateau; C, Central Atlantic Magmatic Province; MR, Maud Rise; M, Magellan Rise; O, Ontong Java Nui, R, Rajmahal, S, Shatsky Rise. Reconstructions are draped on the s10mean tomography model (Doubrovine et al. 2016) together with the 0.9% slow contour (the plume generation zone, PGZ).

Figure 4 Planet Earth according to (a) Courtillot et al. (2003) with three types of hotspots: (1) Primary plumes from the deepest mantle , (2) Secondary plumes originating from the base of the transition zone (above TUZO and JASON) and (3) Superficial “Andersonian” hotspots. (b) Andersonian Earth with no communication between the upper and lower mantle and all hotspots being superficial (see text) (c) The Burkian Earth; A degree-2 Earth governed by the two antipodal TUZO and JASON thermochemical piles and with plumes derived from their margins. Orange colour indicates that the area above them is warmer than the background mantle, and the dashed red-stippled lines indicate that they tend to be overlain by positive geoid anomalies. pBn, post-Bridgmenite; PGZ, Plume Generation Zones; ULVZ, Ultra Low Velocity Zones.

Figure 5 Seismic tomographic SMEAN model (dV_S%) at 2800 km depth (Becker and Boschi 2002) The red line is the 1% slow contour in the SMEAN model (as in Fig. 1c). The white, stippled line marks the central part of the high velocity circumpolar belt through the Arctic, Asia, Australia, Antarctica and the Americas. This belt is presumably the location of descending flow of cold mantle, dominated by subducted slab material. The broad flow directions from the circum-polar belt towards the LLSVP-margins are show by larger arrows with colour gradients illustrating the temperature increase. The location of 27 inferred deep-rooted plumes (primary, clearly resolved and somewhat resolved plumes in French and

Romanowicz, 2015) are marked by small circles and converging arrows indicating inferred directions for the focused D'' flow towards the plume roots. The six plumes marked with purple colour, yellow fill and bold letters have documented compositional asymmetry with higher proportion of recycled oceanic crust on the side towards the LLSVP (see text).

Figure 6 Schematic sections from a circum-polar high V_S-belt to a LLSVP (see text).

Figure 7 (a, b) 2-D cross-sections (parts of the cross-sections are shown in (c)) of shear-wave velocity anomalies across the Hawaii and Iceland hotspots. Broad plumes beneath Hawaii and Iceland extend continuously from the CMB to the uppermost mantle. On the other hand, anomalies are not readily detected in the lower mantle beneath the Yellowstone and Eifel hotspots (French and Romanowicz 2015). (c) Distribution of hotspots (Steinberger 2000) and their calculated surface hotspot motion (Doubrovine et al. 2012) draped on the s10mean shear-wave velocity anomaly model at 2800 km depth (Doubrovine et al. 2016). The s10mean 0.9% slow (thick red line; the plume generation zone in this model) and zero (black line) contours are shown. Velocity anomalies (δV_s) are in percent and red denotes regions with low velocity. Many hotspots appear to overly regions of slower than average shear-wave velocities (notably those associated with TUZO) but there are clear exceptions (e.g. Yellowstone in North America). 20 hotspots thought to be sourced by deep plumes from the core-mantle boundary (primary and clearly resolved plumes in French and Romanowicz, 2015) are shown as large white or black (also identified by Courtillot et al. 2003) circles with red-filling. Others of unknown origin are shown as smaller circles with yellow fillings. (d) As in (c) but only plotting 20 hotspots classified as primary or clearly resolved plumes by French and Romanowicz (2015) and compared with LIPs (squared red boxes with numbers in Myrs) that have been reconstructed from a global moving hotspot frame (maximum age of 125 Ma for those associated with TUZO) and a fixed Pacific hotspot frame from 83-150 Ma (Doubrovine et al. 2012).

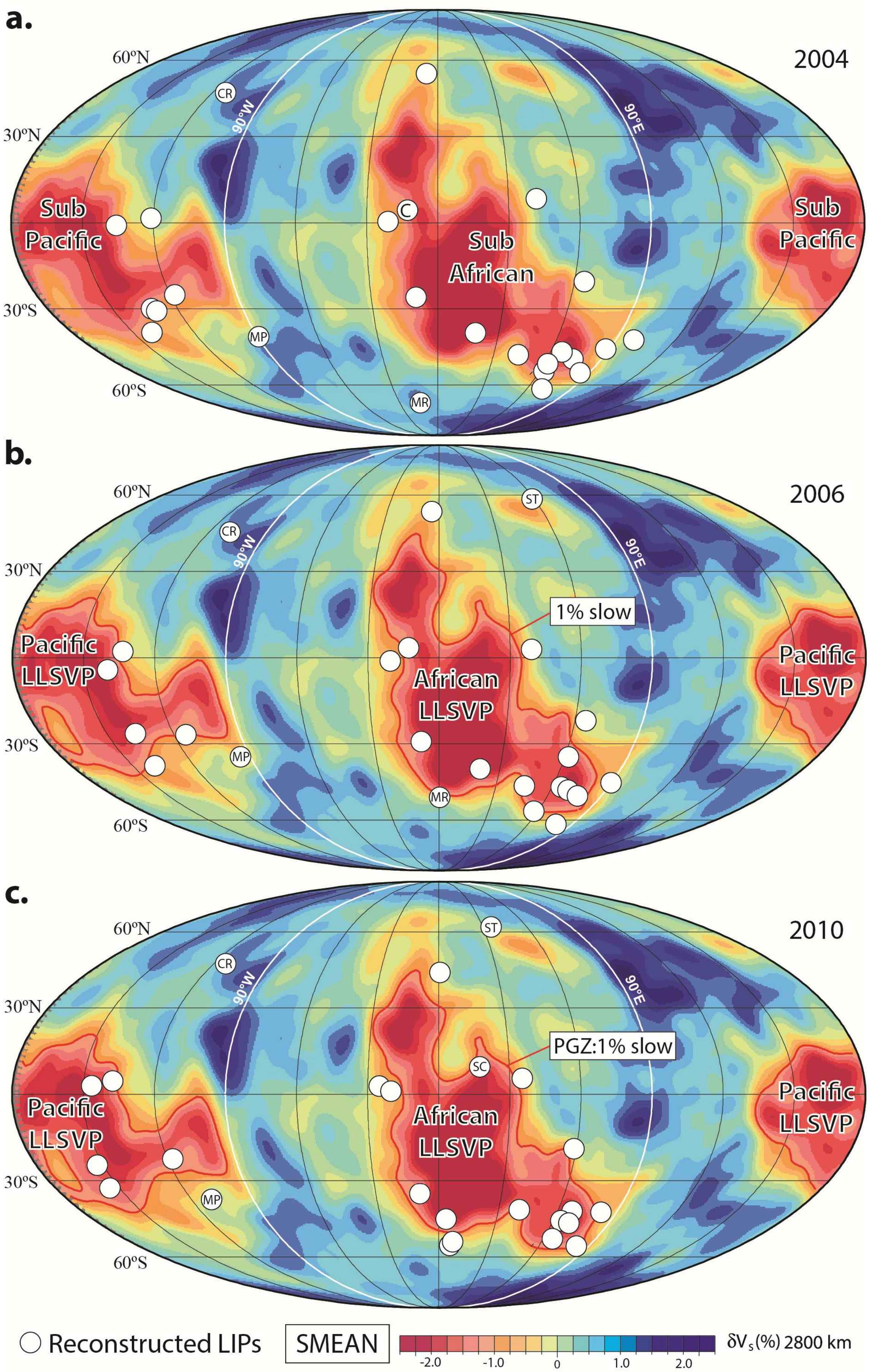

a.
2004
60ºN
30ºN
30ºS
60ºS
CR
90ºW
90ºE
C
MP
MR
Sub Pacific
Sub African
b.
2006
ST
1% slow
Pacific LLSVP
African LLSVP
c.
2010
SC
PGZ:1% slow
Reconstructed LIPs
SMEAN
-2.0
-1.0
0
1.0
2.0
δVs(%) 2800 km

Fig. 1

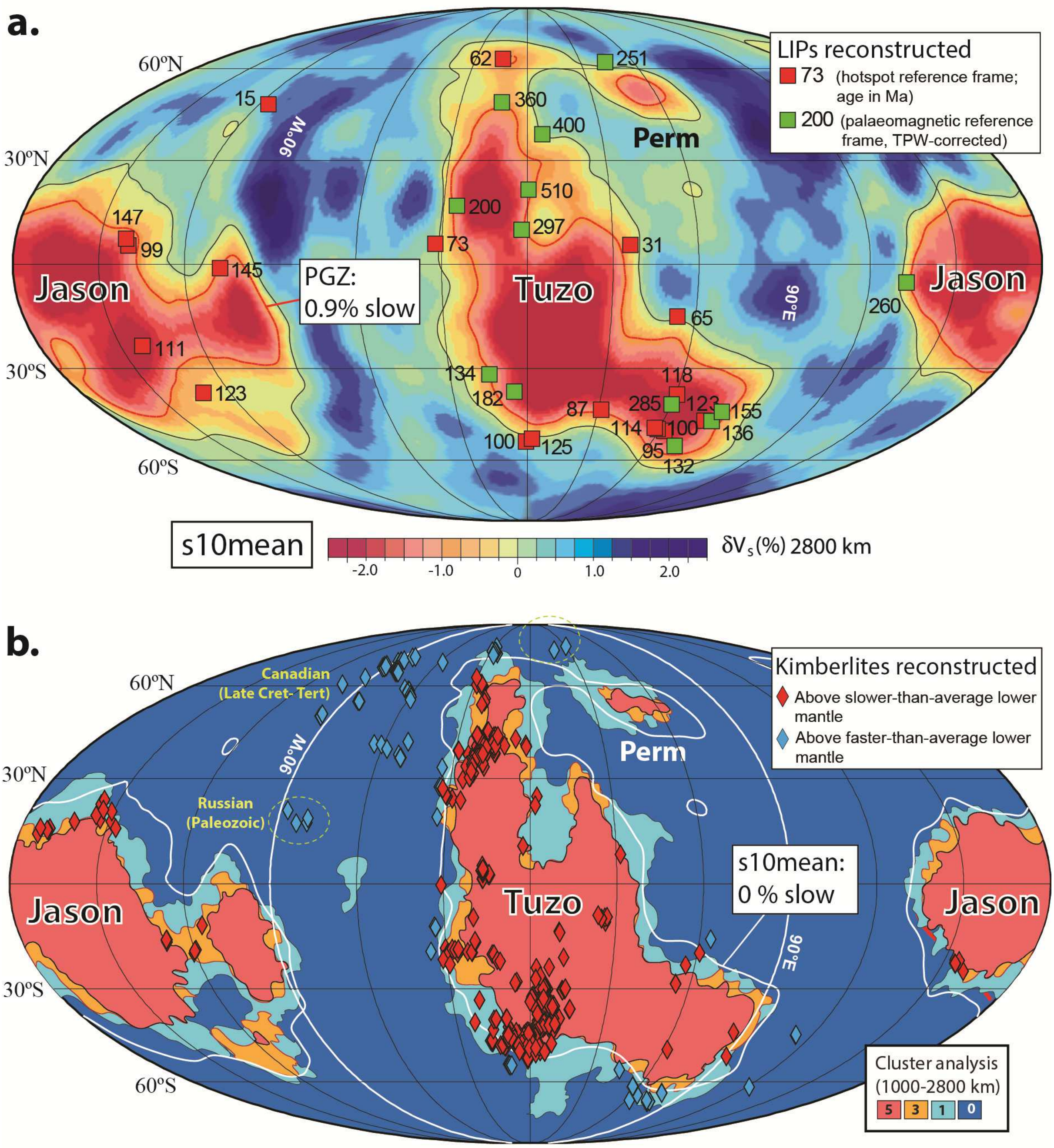
a.
LIPs reconstructed
73 (hotspot reference frame; age in Ma)
200 (palaeomagnetic reference frame, TPW-corrected)
60ºN
30ºN
30ºS
60ºS
90ºW
90ºE
Perm
Jason
Tuzo
PGZ: 0.9% slow
s10mean
δVs(%) 2800 km
-2.0
-1.0
0
1.0
2.0
b.
Kimberlites reconstructed
Above slower-than-average lower mantle
Above faster-than-average lower mantle
Canadian (Late Cret- Tert)
Russian (Paleozoic)
s10mean: 0 % slow
Cluster analysis (1000-2800 km)
5 3 1 0

Fig. 2

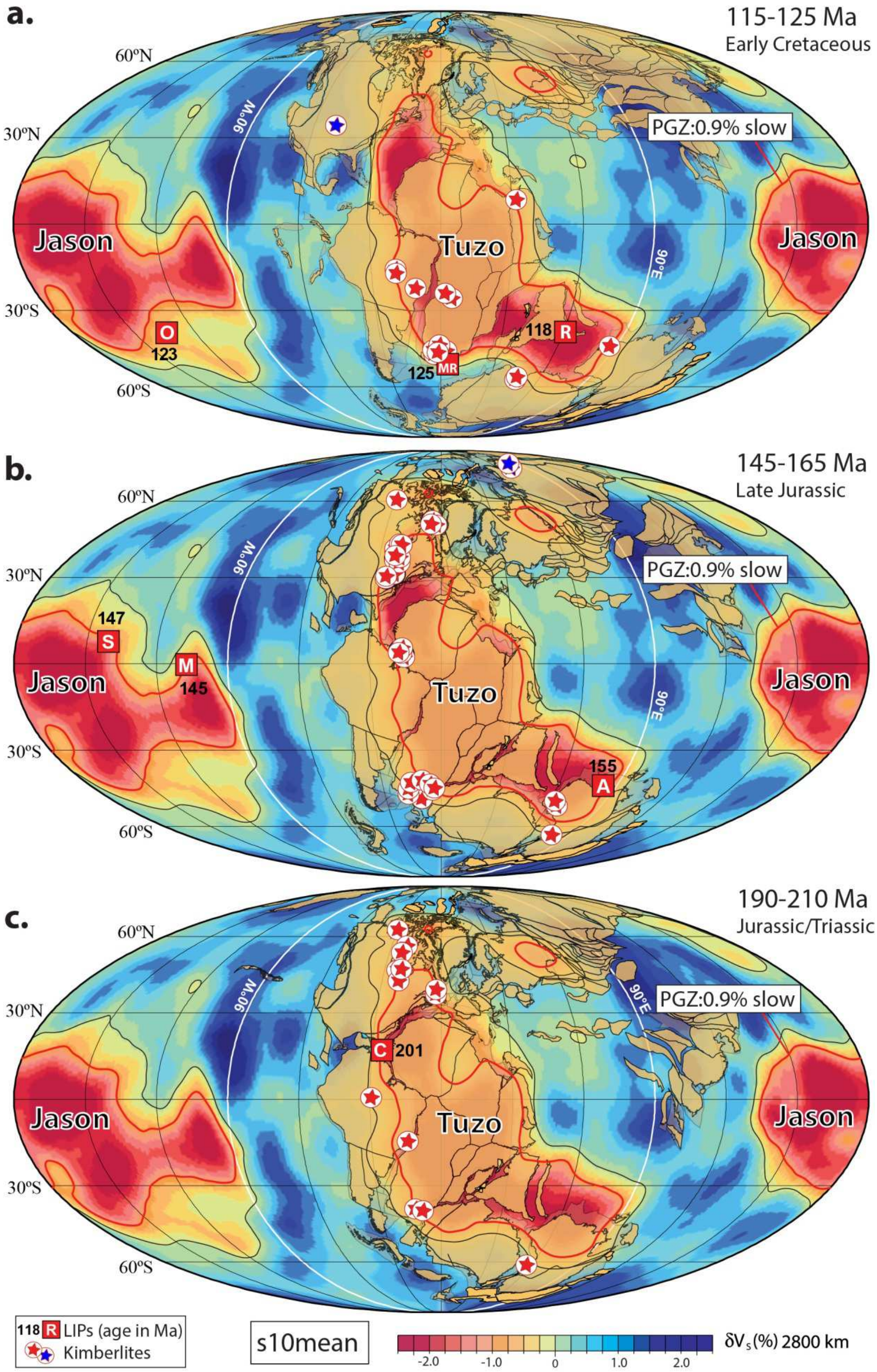
a.
115-125 Ma
Early Cretaceous
60ºN
30ºN
30ºS
60ºS
90ºW
90ºE
PGZ:0.9% slow
Jason
Tuzo
Jason
O
123
125
MR
118
R
b.
145-165 Ma
Late Jurassic
60ºN
30ºN
30ºS
60ºS
90ºW
90ºE
PGZ:0.9% slow
147
S
M
145
Jason
Tuzo
Jason
155
A
c.
190-210 Ma
Jurassic/Triassic
60ºN
30ºN
30ºS
60ºS
90ºW
90ºE
PGZ:0.9% slow
C
201
Jason
Tuzo
Jason
118 R LIPs (age in Ma)
Kimberlites
s10mean
δVs(%) 2800 km
-2.0
-1.0
0
1.0
2.0

Fig. 3

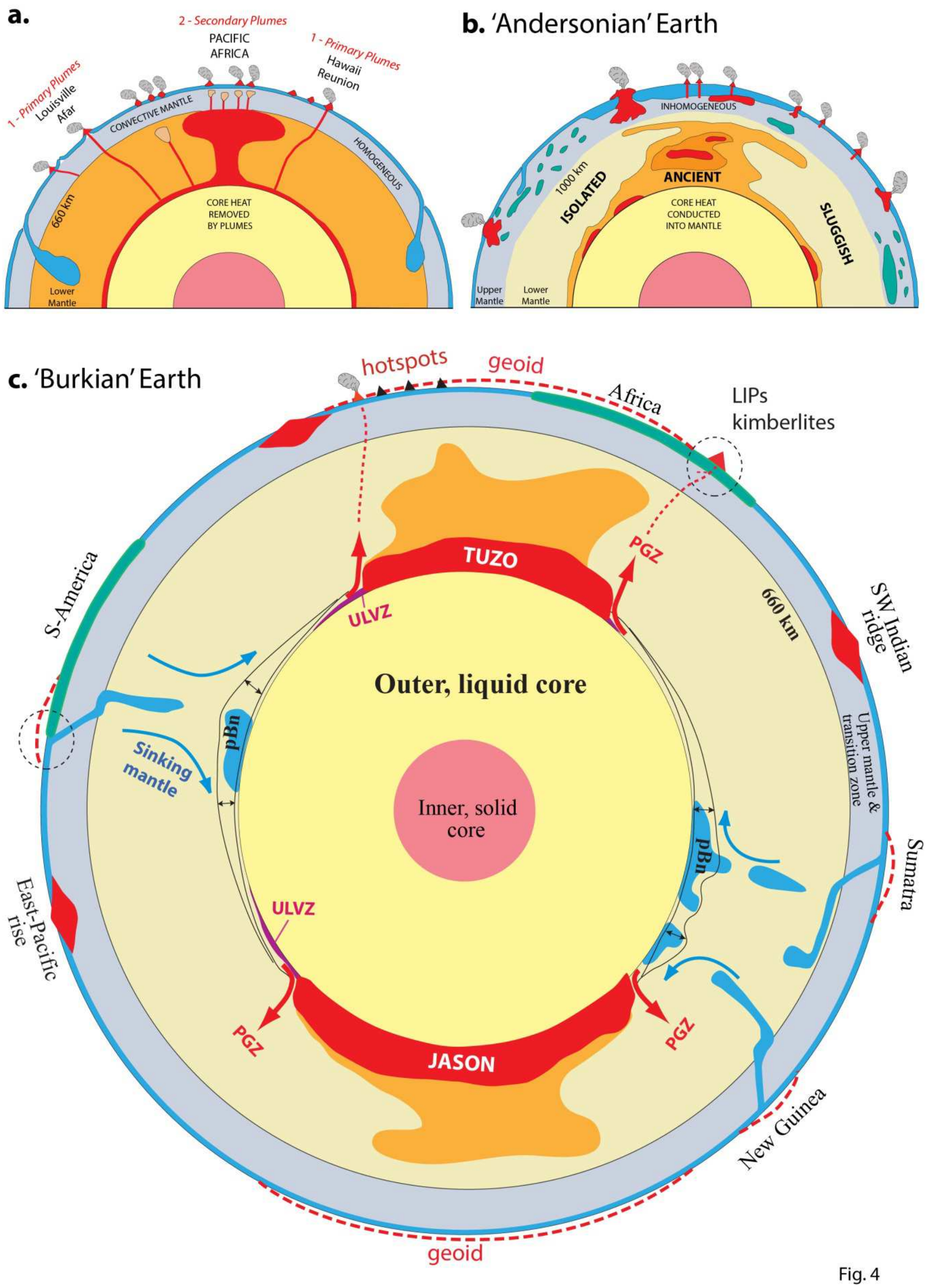
a.
2 - Secondary Plumes
PACIFIC
AFRICA
1 - Primary Plumes
Hawaii
Reunion
1 - Primary Plumes
Louisville
Afar
CONVECTIVE MANTLE
HOMOGENEOUS
660 km
CORE HEAT
REMOVED
BY PLUMES
Lower
Mantle
b. 'Andersonian' Earth
INHOMOGENEOUS
1000 km
ISOLATED
ANCIENT
SLUGGISH
CORE HEAT
CONDUCTED
INTO MANTLE
Upper
Mantle
Lower
Mantle
c. 'Burkian' Earth
hotspots
geoid
Africa
LIPs
kimberlites
PGZ
TUZO
ULVZ
660 km
SW Indian
ridge
S-America
Outer, liquid core
pBn
Sinking
mantle
Upper mantle &
transition zone
Inner, solid
core
pBn
Sumatra
East-Pacific
rise
ULVZ
PGZ
PGZ
JASON
New Guinea
geoid

Fig. 4

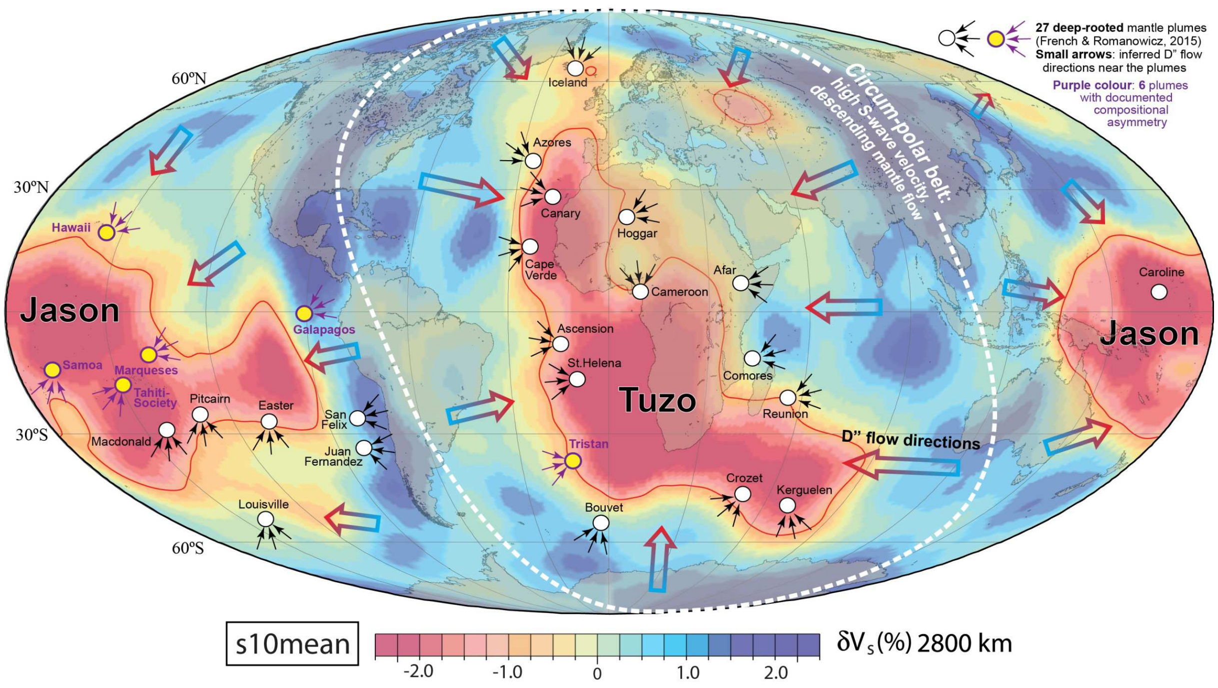
27 deep-rooted mantle plumes (French & Romanowicz, 2015)
Small arrows: inferred D" flow directions near the plumes
Purple colour: 6 plumes with documented compositional asymmetry
Circum-polar belt: high S-wave velocity, descending mantle flow
60ºN
30ºN
30ºS
60ºS
Jason
Tuzo
Jason
Iceland
Azores
Canary
Hoggar
Cape Verde
Cameroon
Afar
Ascension
St.Helena
Comores
Reunion
Tristan
Crozet
Kerguelen
Bouvet
Caroline
Hawaii
Galapagos
Samoa
Marqueses
Tahiti-Society
Pitcairn
Easter
Macdonald
San Felix
Juan Fernandez
Louisville
D" flow directions
s10mean
-2.0
-1.0
0
1.0
2.0
δV$_S$(%) 2800 km

Fig. 5

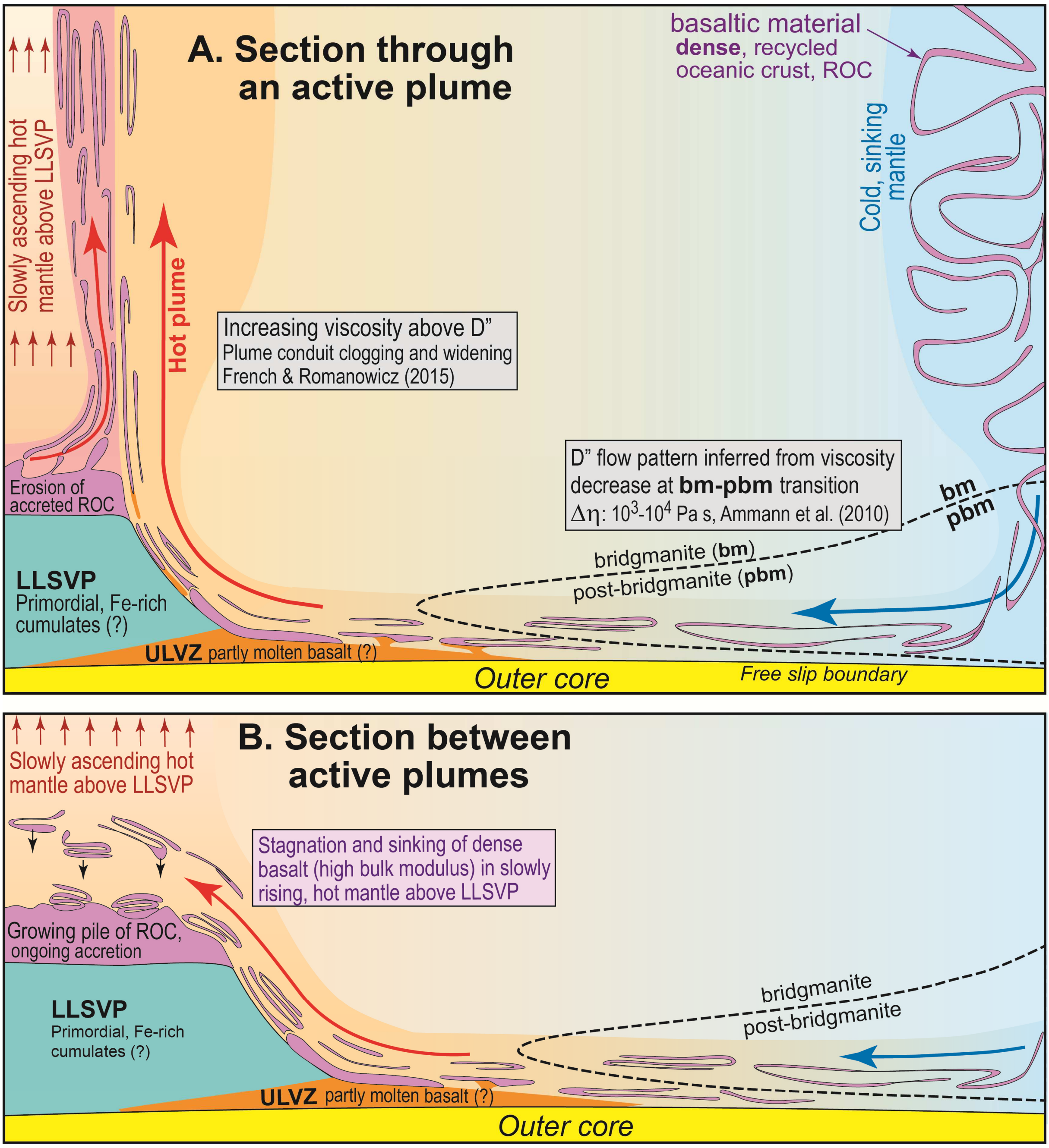

A. Section through an active plume
basaltic material
dense, recycled oceanic crust, ROC
Cold, sinking mantle
Slowly ascending hot mantle above LLSVP
Hot plume
Increasing viscosity above D”
Plume conduit clogging and widening
French & Romanowicz (2015)
D” flow pattern inferred from viscosity decrease at bm-pbm transition
Δη: 10^3-10^4 Pa s, Ammann et al. (2010)
bm
pbm
Erosion of accreted ROC
LLSVP
Primordial, Fe-rich cumulates (?)
bridgmanite (bm)
post-bridgmanite (pbm)
ULVZ partly molten basalt (?)
Outer core
Free slip boundary
B. Section between active plumes
Slowly ascending hot mantle above LLSVP
Stagnation and sinking of dense basalt (high bulk modulus) in slowly rising, hot mantle above LLSVP
Growing pile of ROC, ongoing accretion
LLSVP
Primordial, Fe-rich cumulates (?)
bridgmanite
post-bridgmanite
ULVZ partly molten basalt (?)
Outer core

Fig. 6

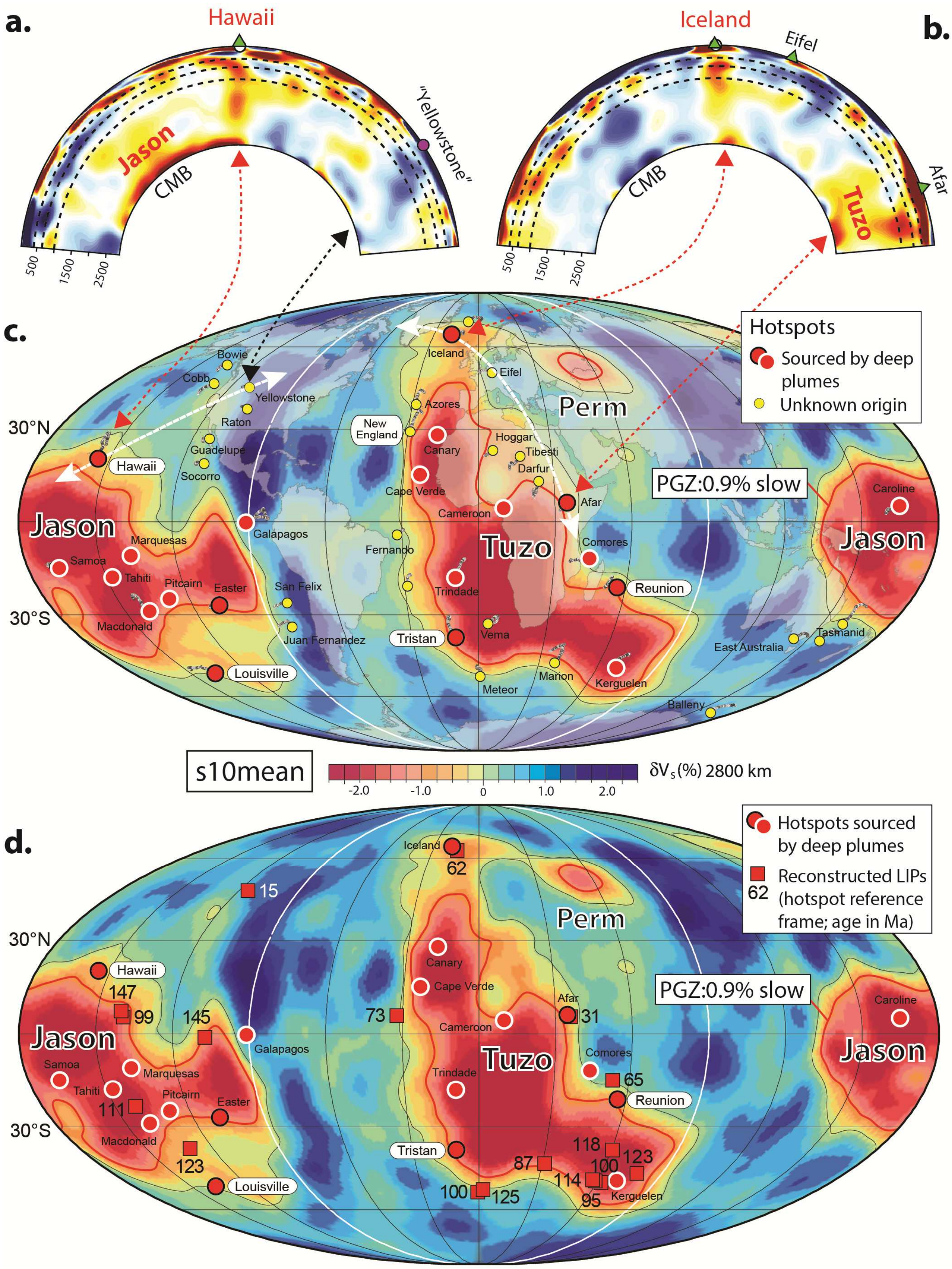
a.
Hawaii
Jason
CMB
"Yellowstone"
500
1500
2500
b.
Iceland
Eifel
Afar
Tuzo
CMB
500
1500
2500
c.
Hotspots
Sourced by deep plumes
Unknown origin
Bowie
Cobb
Yellowstone
Raton
Guadelupe
Socorro
30°N
Hawaii
Jason
Marquesas
Samoa
Tahiti
Pitcairn
Easter
Macdonald
30°S
Louisville
Galapagos
San Felix
Juan Fernandez
Iceland
Eifel
Azores
New England
Canary
Cape Verde
Hoggar
Tibesti
Darfur
Afar
Cameroon
Fernando
Tuzo
Trindade
Tristan
Vema
Meteor
Marion
Kerguelen
Comores
Reunion
Perm
PGZ:0.9% slow
Caroline
Jason
East Australia
Tasmanid
Balleny
s10mean
δV$_s$(%) 2800 km
-2.0
-1.0
0
1.0
2.0
d.
Hotspots sourced by deep plumes
Reconstructed LIPs (hotspot reference frame; age in Ma)
62
Iceland
62
15
Perm
30°N
Hawaii
147
99
145
73
Canary
Cape Verde
Afar
31
Cameroon
PGZ:0.9% slow
Caroline
Jason
Galapagos
Tuzo
Comores
Samoa
Marquesas
Trindade
65
Tahiti
Pitcairn
Easter
111
Reunion
30°S
Macdonald
123
Tristan
118
123
87
100
114
95
Kerguelen
100
125
Louisville

Fig. 7